City University, 29 June 2001

Three Dimensional Numerical Simulation of Screw Compressor Processes as a Design Tool

Ahmed Kovačević

Centre for Positive Displacement Compressor Technology
City University London, UK

Screw compressor

- 100 million positive displacement compressors are produced annually
- A great proportion of all power generated is used to drive compressors
- Majority of them today are of screw type
- These are positive displacement rotary machines
- Working chamber formed by the rotors and a casing
- Trapped volume depends on the angle of rotation

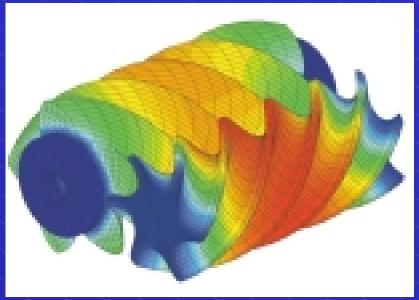

- Complex geometry configuration
- Moving parts rotate and slide causing the volume to stretch

Performance affected by:

- Leakage through the gaps,
- Oil distribution,
- Thermal and transport properties of working fluids,
- Distortion of rotors and housing,
- Two phase, separation and particle flows.

The twin screw compressor-principle of operation

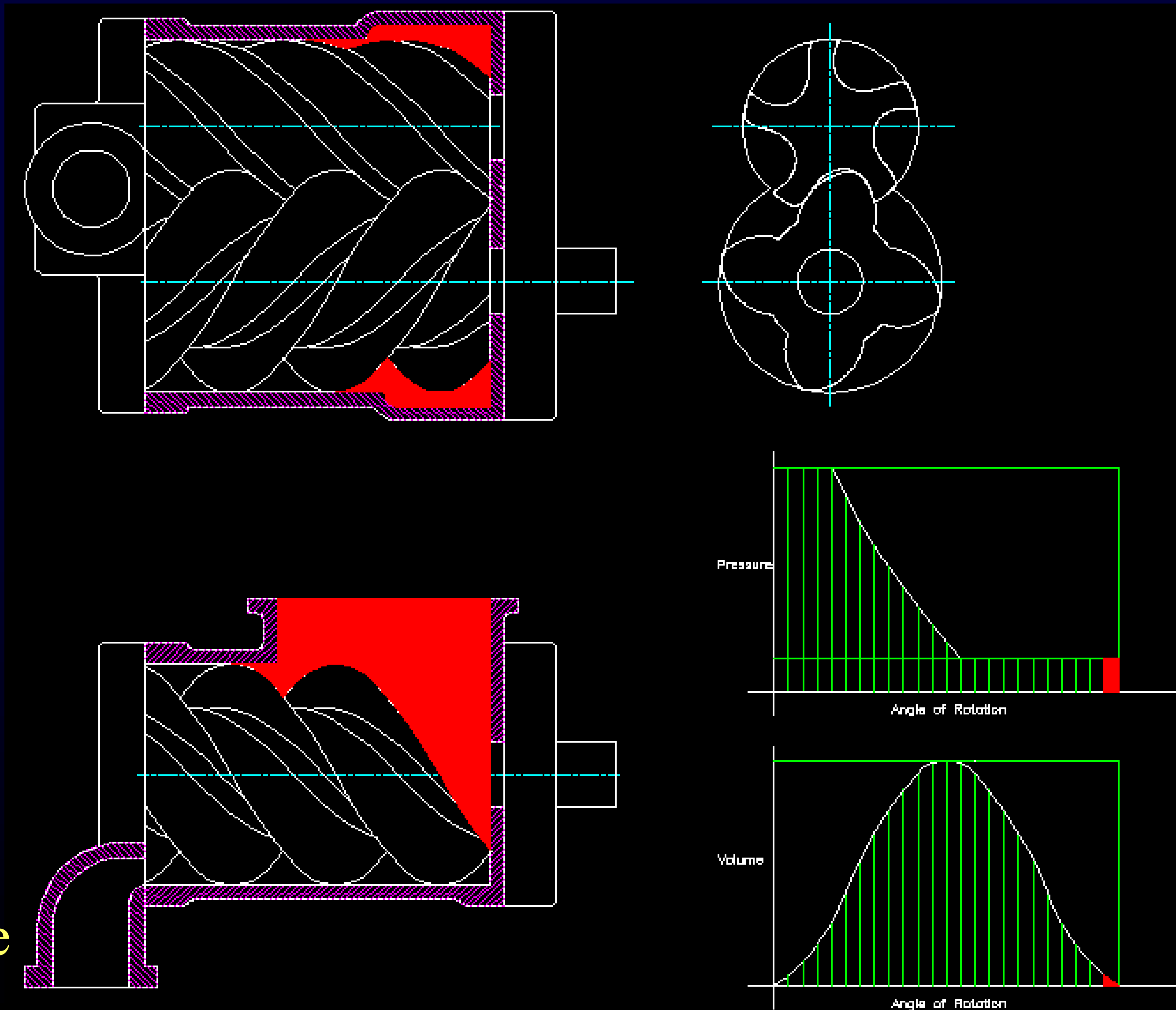

Female

Male

Suction

Discharge

Flow and thermodynamic simulation

Screw Compressor performance is reasonably well predicted by ONE-DIMENSIONAL models. These assume that:

•Both main and leakage flows are one dimensional,

•The oil passes through the machine in contact with the housing,

•Dynamic inlet and outlet effects are negligible.

•Effects of temperature distortions are negligible,

The design of industrial screw compressors needs

3-D Flow and stress calculations

• Reliable performance prediction with:
• calculation of dynamic losses and leakages,
• effects of two-phase flow and oil distribution,
• vapour-liquid separation in complex geometry

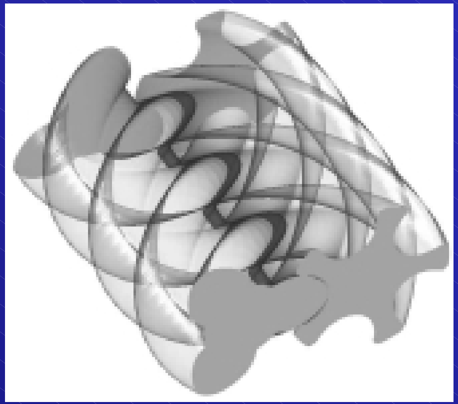

CFD - Computational Fluid Dynamics
FSI - Fluid – Solid Interaction

CFD and Screw compressors

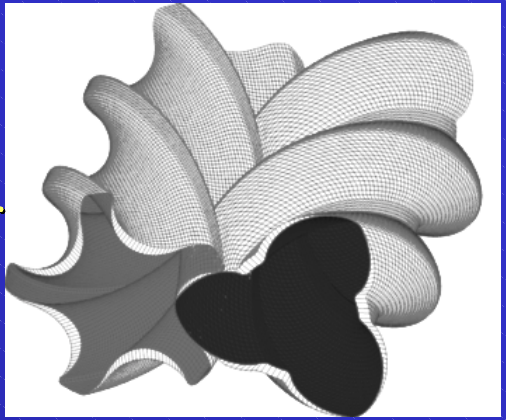

- Large number of publications in the CFD field.
- Little published in CFD for screw compressor flow.
- Complexity of their geometry and flow patterns.
- Many CFD solvers with useful features.
- AIM - to enable use of any CFD solver which has:
  - Finite volume method,
  - Governing equation of mass, momentum, energy and species,
  - Block-structured hexahedral mesh,
  - Moving mesh domains,
  - Sliding boundaries,
  - Explicit and implicit cell connectivity,
  - Accessible user subroutines.
- Novel features are introduced in the analytical mesh generation process:
  - advanced analytical grid generation,
  - Hermite transfinite interpolation and multidimensional stretching functions,
  - multiparameter boundary adaptation orthogonalisation, smoothing and regularity check.
- Input file and user subroutines prepared automatically for a CFD code to:
  - read vertices, cells and regions,
  - calculate energy, mass and momentum sources of liquid phase and oil,
  - read boundary and initial conditions
  - maintain constant pressures in receivers
  - calculate properties of real fluids.

Grid generation

- Grid topology strongly affects accuracy, efficiency and ease of generation of the proper solution.
- Full structured block generated hexahedral 3D-O mesh
- Screw compressor domain divided into sub-domains:

- Male rotor

- Female rotor

- End clearances

Rotor connections, clearances, leakage paths

- Suction port

- Discharge port

- Suction and discharge receivers

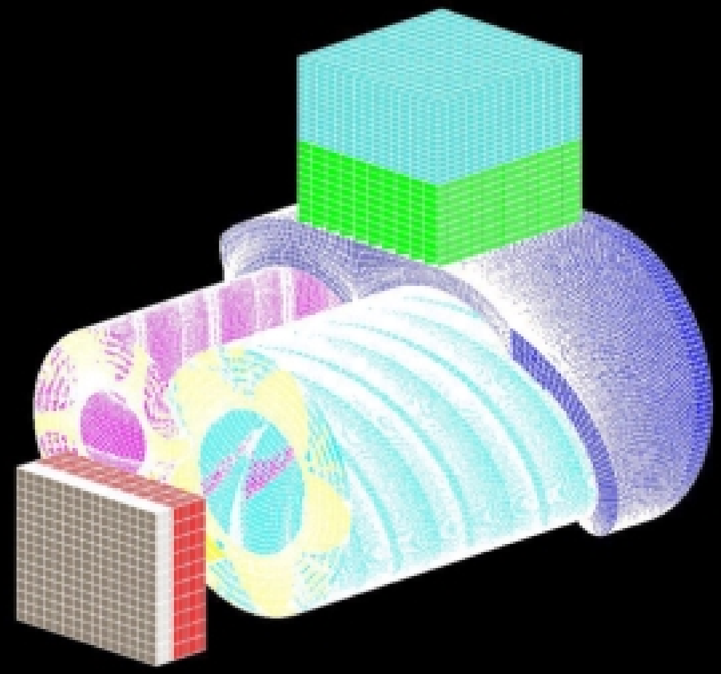

Algebraic transfinite interpolation, multiparameter stretching functions, orthogonalization, smoothing and regularity check.

Distribution of boundary points

- Basis - The rack generating procedure with strong mathematical background.
- A rack is a rotor with an infinite radius and the shortest lobe length
- Divide entire working domain in two parts, one belonging to the male and the other to the female rotor.

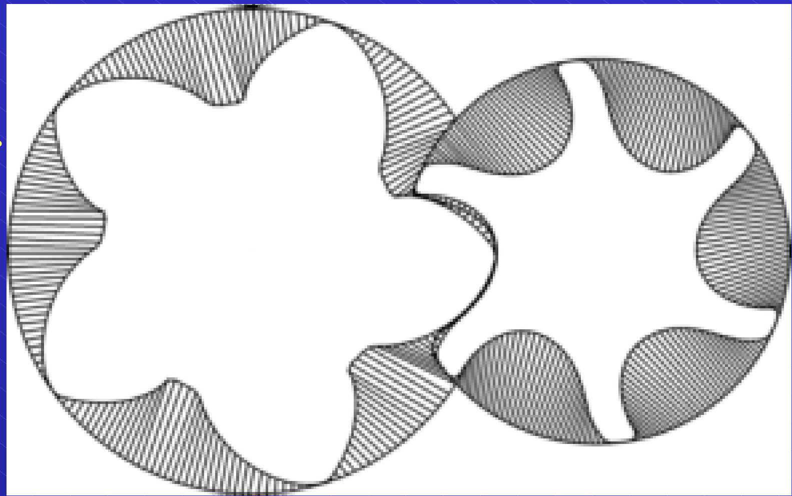

•**SCORPATH** – **S**crew **C**ompressor **O**ptimal **R**otor **P**rofiling **A**nd **T**hermodynamics

- Discretization starts with only few data:
  - *X* and *Y* rack lobe coordinates, number of teeth on rotors, rotor axis distance, clearance distribution, prescribed number of nodes.

Rotor generated from a defined rack

The rack enclosed with an outer circle

Point distribution procedure applied with multidimensional adaptation

Derive output: Boundaries of 2-D structured "O" mesh

Same procedure repeated for all required cross sections

Transfinite interpolation

The analytical transfinite interpolation method has been applied to obtain coordinates of internal point. For a 2-D domain it reads:

$$x(\xi,\eta) = X_1(\xi,\eta)\alpha_1(\xi) + X_2(\xi,\eta)\alpha_2(\xi)$$
$$y(\xi,\eta) = Y_1(\xi,\eta)\beta_1(\eta) + Y_2(\xi,\eta)\beta_2(\eta)$$

Application of different blending functions leads to different solutions.

Hermite interpolation - 4 blending functions:

$$x(\xi,\eta) = x'(\xi,\eta) + \Delta x(\xi,\eta)$$
$$y(\xi,\eta) = y'(\xi,\eta) + \Delta y(\xi,\eta)$$

$$x'(\xi,\eta) = X_1(\xi)h_1(\eta) + X_2(\xi)h_2(\eta) + \frac{\partial x(\xi,\eta=0)}{\partial\eta}h_3(\eta) + \frac{\partial x(\xi,\eta=1)}{\partial\eta}h_4(\eta)$$

$$y'(\xi,\eta) = Y_1(\xi)h_1(\eta) + Y_2(\xi)h_2(\eta) + \frac{\partial y(\xi,\eta=0)}{\partial\eta}h_3(\eta) + \frac{\partial y(\xi,\eta=1)}{\partial\eta}h_4(\eta)$$

$$\Delta x(\xi,\eta) = (X_3 - X'_3)h_5(\xi) + (X_4 - X'_4)h_6(\xi) + \left(\frac{\partial x(\xi=0,\eta)}{\partial\xi} - \frac{\partial x'(\xi=0,\eta)}{\partial\xi}\right)h_7(\xi) + \left(\frac{\partial x(\xi=1,\eta)}{\partial\xi} - \frac{\partial x'(\xi=1,\eta)}{\partial\xi}\right)h_8(\xi)$$

$$\Delta y(\xi,\eta) = (Y_3 - Y'_3)h_5(\xi) + (Y_4 - Y'_4)h_6(\xi) + \left(\frac{\partial y(\xi=0,\eta)}{\partial\xi} - \frac{\partial y'(\xi=0,\eta)}{\partial\xi}\right)h_7(\xi) + \left(\frac{\partial y(\xi=1,\eta)}{\partial\xi} - \frac{\partial y'(\xi=1,\eta)}{\partial\xi}\right)h_8(\xi)$$

$$h_1 = 2\eta^3 - 3\eta^2 + 1,\ \ h_2 = -2\eta^3 + 3\eta^2$$
$$h_3 = \eta^3 - 2\eta^2 + \eta,\ \ h_1 = \eta^3 - \eta^2$$

$$h_5 = 2\xi^3 - 3\xi^2 + 1,\ \ h_6 = -2\xi^3 + 3\xi^2$$
$$h_7 = \xi^3 - 2\xi^2 + \xi,\ \ h_8 = \xi^3 - \xi^2$$

Transfinite interpolation

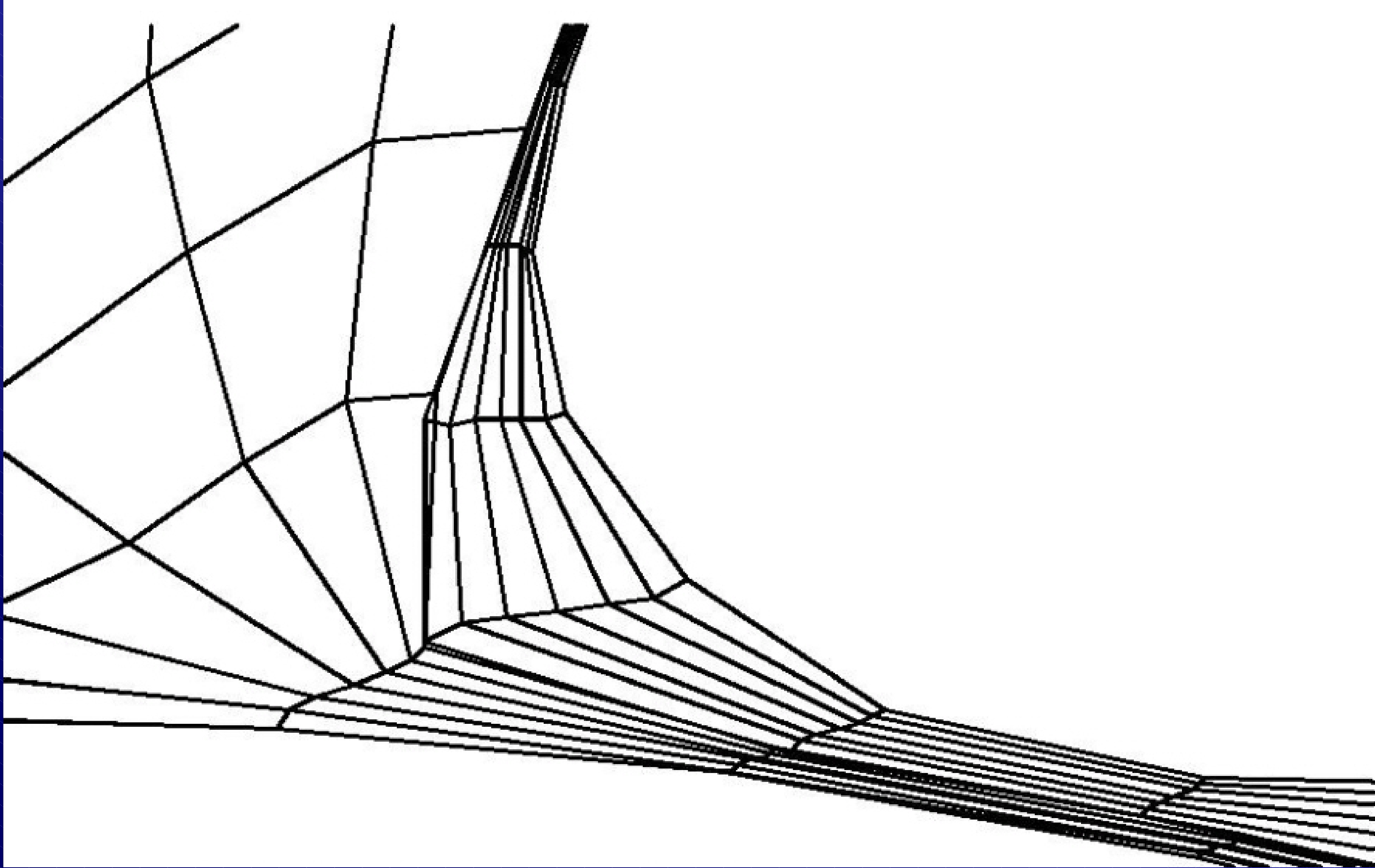

SCORG – Stand alone CFD pre-processor

SCORG
Screw COmpressor Rotor Geometry grid generator

Rot (nang,nast,naen,irot)

Rack (nang,nada)

Distr (irot,ka,idi,ma)

Mesh (nang,nada,irot,ntr,imesh)

Inlet (irot,fi1c,radd,nn1,nn2,
irax,imesh,nang)

Outlet (irot,fi1c)

Prep (radd,nd,om1,pinl,pout,
nang,irax)

Transf (imin,imax,jmin,jmax,ntr)

Simple (imin,imax,jmin,jmax,ntr)

Ortho (imin,imax,jmin,jmax)

Gridsm (imin,imax,jmin,jmax,ir)

Grireg (imin,imax,jmin,jmax,ir)

Smooth (ra,ar,fip,fik,dfi,ns,nsp)

Names (iang)
Check (npos,jro,ynew)
Circ (r,nt,a,fip,fik,dfi,jhoce)
Equal (mp,m,np,n,j)
Celreg (i,j)

Moving mesh generated by SCORG

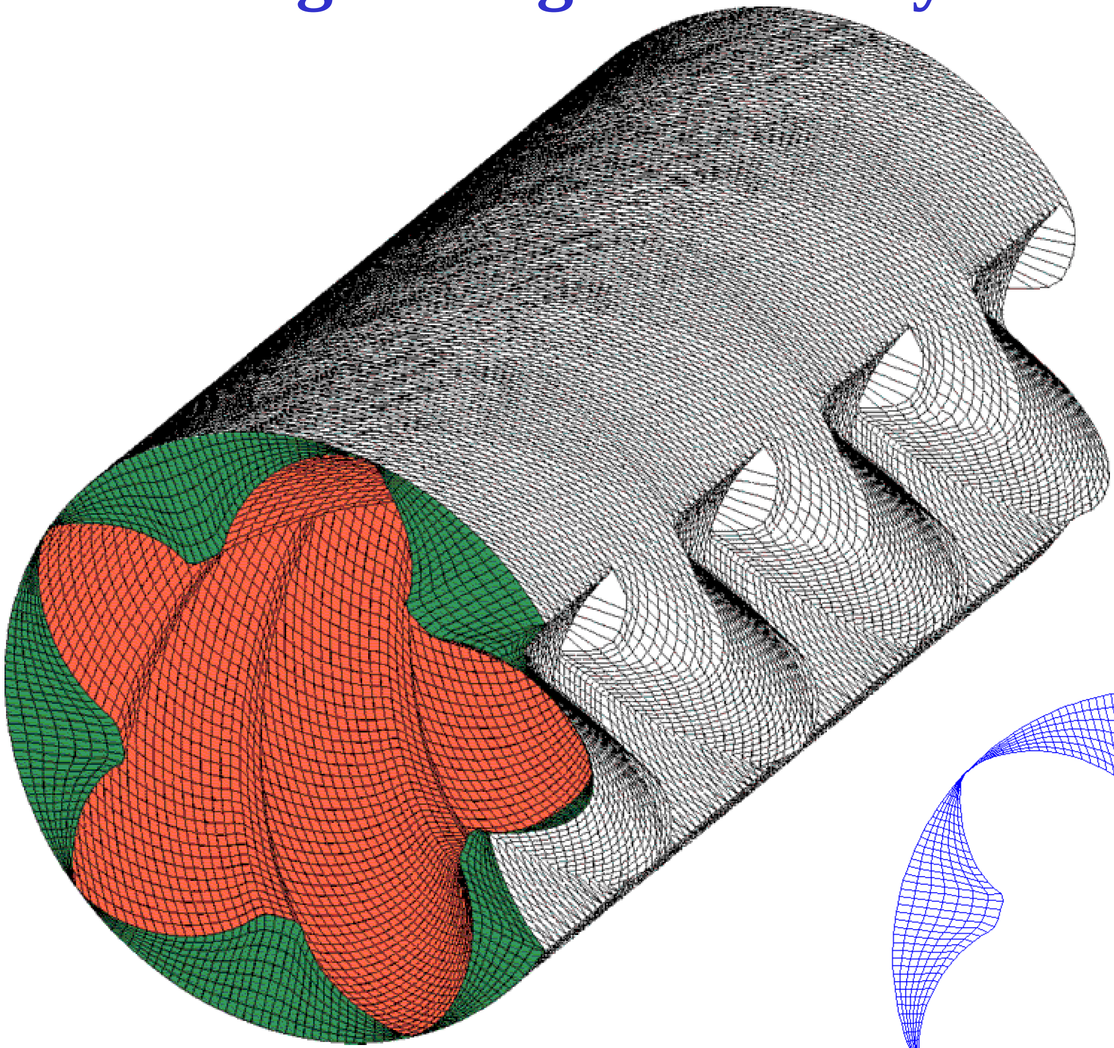

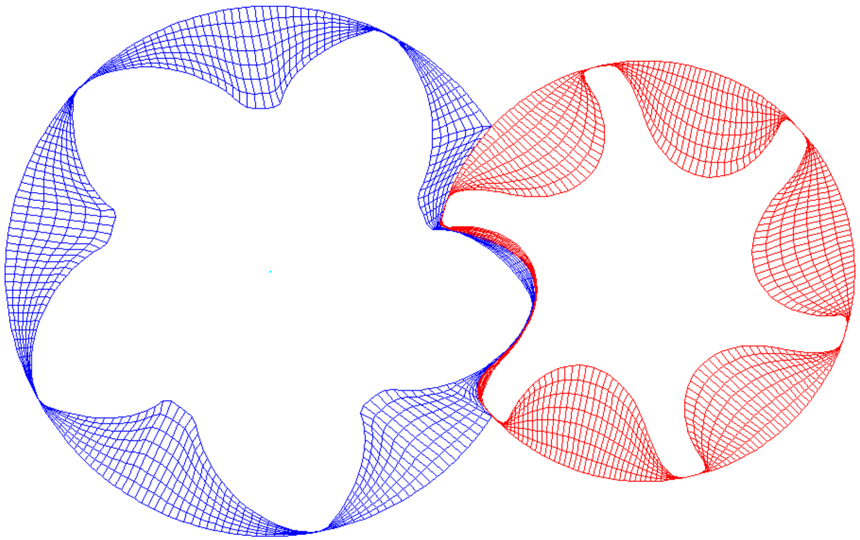

Screw Compressor CFD calculations

Mathematical model for screw compressor is based on conservation laws of continuity, momentum, energy, species and space:

$$\frac{d}{dt}\int_V \rho dV + \int_S \rho(\mathbf{v}-\mathbf{v}_s)\cdot d\mathbf{s} = 0$$

$$\rho = \rho(p,T), \quad e = e(p,T)$$

$$\frac{d}{dt}\int_V \rho \mathbf{v} dV + \int_S \rho \mathbf{v}(\mathbf{v}-\mathbf{v}_s)\cdot d\mathbf{s} = \int_S \mathbf{T}\cdot d\mathbf{s} + \int_V \mathbf{f}_b dV$$

$$\mathbf{T} = 2\mu\dot{\mathbf{D}} - \frac{2}{3}\mu \,\mathrm{div}\, \mathbf{v}\mathbf{I} - p\mathbf{I}$$

$$\frac{d}{dt}\int_V \rho h dV + \int_S \rho h(\mathbf{v}-\mathbf{v}_s)\cdot d\mathbf{s} =$$

$$\int_S \mathbf{q}_h \cdot d\mathbf{s} + \int_V s_h dV + \int_V (\mathbf{v}\cdot \mathrm{grad}\, p + \mathbf{S} : \mathrm{grad}\, \mathbf{v}) dV - \int_S p\mathbf{v}_s \cdot d\mathbf{s} + \frac{d}{dt}\int_V p dV$$

$$\mathbf{q}_h = \kappa \,\mathrm{grad}\, T$$

$$\frac{d}{dt}\int_V \rho c_o dV + \int_S \rho c_o(\mathbf{v}-\mathbf{v}_s)\cdot d\mathbf{s} = \int_S \mathbf{q}_{c_o}\cdot d\mathbf{s} + \int_V S_{c_o} dV$$

$$\mathbf{q}_{c_o} = \rho D_o \,\mathrm{grad}\, c_o$$

$$\frac{d}{dt}\int_V dV - \int_S \mathbf{v}_s \cdot d\mathbf{s} = 0$$

Accompanied by the equations of k-ε turbulence model and equation of state to form closed system.

$$\frac{d}{dt}\int_V \rho k dV + \int_S \rho k(\mathbf{v}-\mathbf{v}_s)\cdot d\mathbf{s} = \int_S \mathbf{q}_k \cdot d\mathbf{s} + \int_V (P - \rho\varepsilon) dV,$$

$$\frac{d}{dt}\int_V \rho\varepsilon dV + \int_S \rho\varepsilon(\mathbf{v}-\mathbf{v}_s)\cdot d\mathbf{s} = \int_S \mathbf{q}_\varepsilon \cdot d\mathbf{s} + \int_V \left(C_1 P\frac{\varepsilon}{k} - C_2\rho\frac{\varepsilon^2}{k} + C_3\rho\varepsilon\nabla\cdot\mathbf{v}\right) dV$$

Thermodynamic properties of real fluids

-*p*-*v*-*T* equation
compressibility factor *z*

$$\frac{p}{\rho} = z \cdot RT = z(p) \cdot RT$$

-*z* is assumed to change linearly
with pressure err<2%

$$z = p \cdot B_1 + B_2$$

- Antoine equation for saturation
temperature

$$T_{sat} = \frac{A_2}{A_1 - \log p}$$

- Clapeyron equation for latent heat

$$h_L = T \cdot \left(\frac{1}{\rho_v} - \frac{1}{\rho_l} \right) \cdot \frac{dP_{sat}}{dT_{sat}}$$

- Specific heat for constant pressure

$$c_{pv} = C_0 + C_1 \cdot T + C_2 \cdot T^2 + C_2 \cdot T^3$$

- Density of mixture

$$\rho = \frac{1}{\frac{1 - co_2}{\rho_v} - \frac{co_2}{\rho_l}}$$

- Coefficient in the pressure correction
equation

$$C_\rho = \left(\frac{d\rho}{dp} \right)_T = \left(\frac{1}{zRT} - \frac{\rho_v \cdot b_1}{z} \right) \cdot \frac{\rho_v}{\rho}$$

Multiphase flow

$$\frac{d(m_o h_o)}{dt} = m_o \frac{dh_o}{dt} + h_{ol} \frac{dm_o}{dt} = \dot{Q}_{con} + \dot{Q}_{mass}$$

- **Oil** is assumed to be a passive 'species'
- Mass calculated from the concentration

$$\dot{Q}_{con} = m_o C_{p_o} \frac{dT}{dt} \approx m_o C_{p_o} \frac{T^k - T^{k-1}}{\delta t}$$

- Oil drag force influence concentration

$$\mathbf{f}_{drag} = -\frac{1}{2} \rho A_o C_{drag} \left| \mathbf{v}_o - \mathbf{v} \right| (\mathbf{v}_o - \mathbf{v})$$

- **Liquid phase** is a active 'species'
- Energy source influence of the liquid phase

$$\dot{Q}_{mass} = h_L \frac{dm_L}{dt} \approx h_L \frac{\Delta m_L}{\delta t} = h_L \frac{m_{ol} - m_{ol}^{s}}{\delta t} = h_L \dot{m}_L$$

- Mass source mass transfer

$$\dot{m}_L = \frac{m \cdot C_{pm} \cdot (T - T_s)}{h_L}$$

Boundary conditions

- Wall boundaries with wall functions are introduced on the housing and rotors.

- Compressor is positioned between suction and discharge receivers of relatively small volume.

- Inlet & outlet receivers and oil port treated as boundary domains:

- Mass equation corrected by mass source to maintain constant pressure

$$\dot{m}_{add} = \left(\frac{dm}{dt}\right)_{p=const} \approx \frac{p_{const} - p}{p_{const}} \cdot \frac{V \cdot \rho}{\delta t}$$

- Energy equation corrected by energy source to update energy balance

$$\dot{Q}_{add} = h_{add}\left(\frac{d\dot{m}_{add}}{dt}\right)_{p=const} = \dot{m}_{add} \cdot h_{add}$$

Screw Compressor performance

- Volume flow (inlet and outlet)

$$\dot{V} = 60 \cdot \sum_{t=t_{start}}^{t_{end}} \dot{V}_f^{(t)} \; \left[m^3/\min\right], \qquad \dot{V}_f^{(t)} = \sum_{i=1}^{I} v_{fi} S_{fi}$$

- Mass flow (inlet, outlet and oil)

$$\dot{m} = \sum_{t=t_{start}}^{t_{end}} \dot{V}_f^{(t)} \cdot \bar{\rho}^{(t)} \quad [kg/\sec]$$

- Boundary forces

$$F_x = p_b * A_{xb}; \quad F_y = p_b * A_{yb}; \quad F_z = p_b * A_{zb}$$

- Restraint Forces and Torque

$$F_{rS} = \sum_{i=1}^{I} F_{rS}(i), [N]; \qquad F_{rD} = \sum_{i=1}^{I} F_{rD}(i), [N]$$

$$F_a = \sum_{i=1}^{I} F_a(i), [N]; \qquad T = \sum_{i=1}^{I} T(i), [Nm]$$

- Compressor shaft power

$$P = 2 \cdot \pi \cdot n \cdot (T_M + T_F) \quad [W]$$

- Specific power

$$P_{spec} = {}^{P}\!/_{\dot{V}} \cdot 1000 \quad \left[{}^{kW}\!/_{m^3 \min}\right]$$

- Efficiency
  Volumetric and adiabatic

$$\eta_v = {}^{\dot{V}}\!/_{V_d}; \qquad \eta_i = {}^{P_{ad}}\!/_{P}$$

Dry compressor – comparison

Same housing and rotor configuration - different rotor profiles:

Configuration 4/6, d_1= 142.380 mm, d_2= 135.820 mm, a= 108.4 mm

l=252.0 mm, l/d=1.77, wrap=248.4 deg, Clearances 150 μm

Speed 6000 rpm, P_{inl}= 1 bar, P_{out} = 3 bar

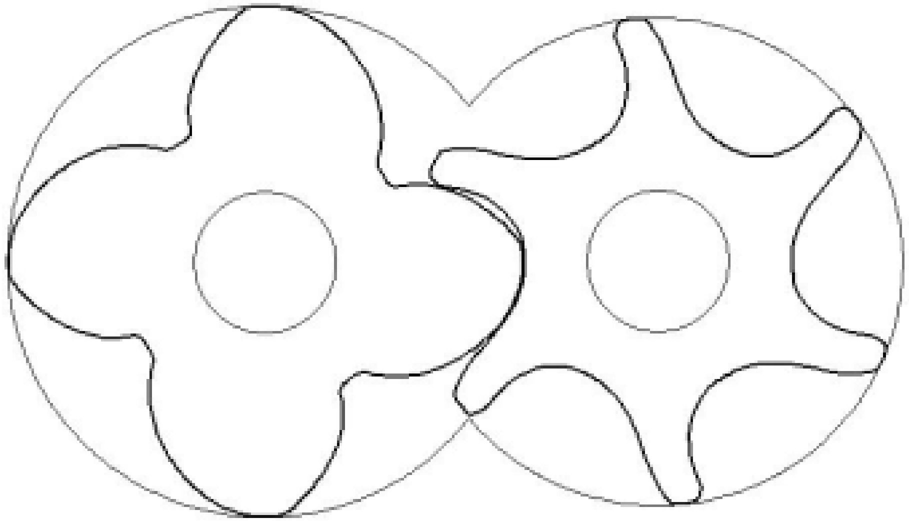

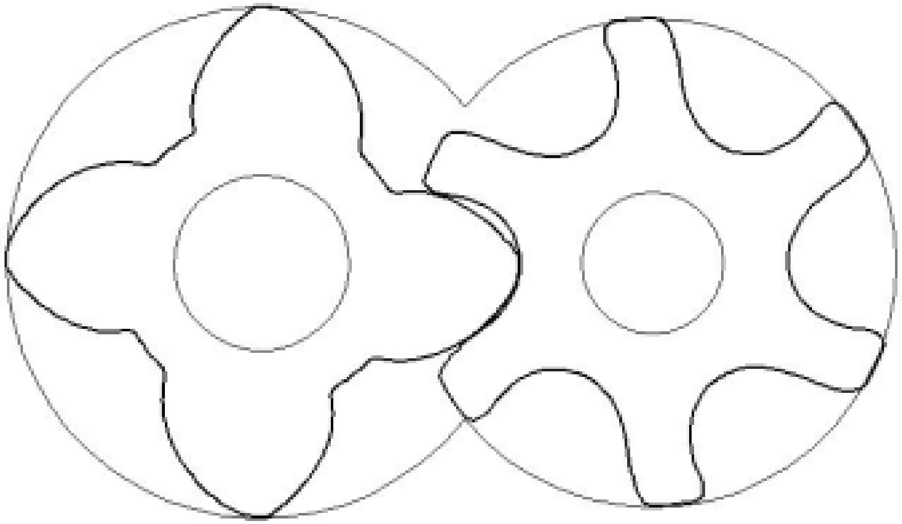

Case 1

327090

Numerical cells

35 time steps

in a cycle

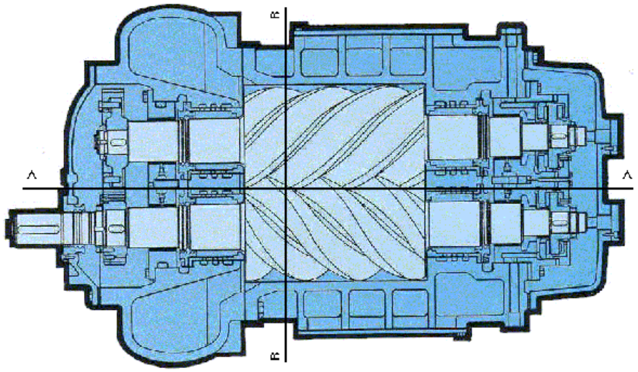

Case 2

406570

Numerical cells

40 time steps

in a cycle

Dry compressor – velocities in Z plane

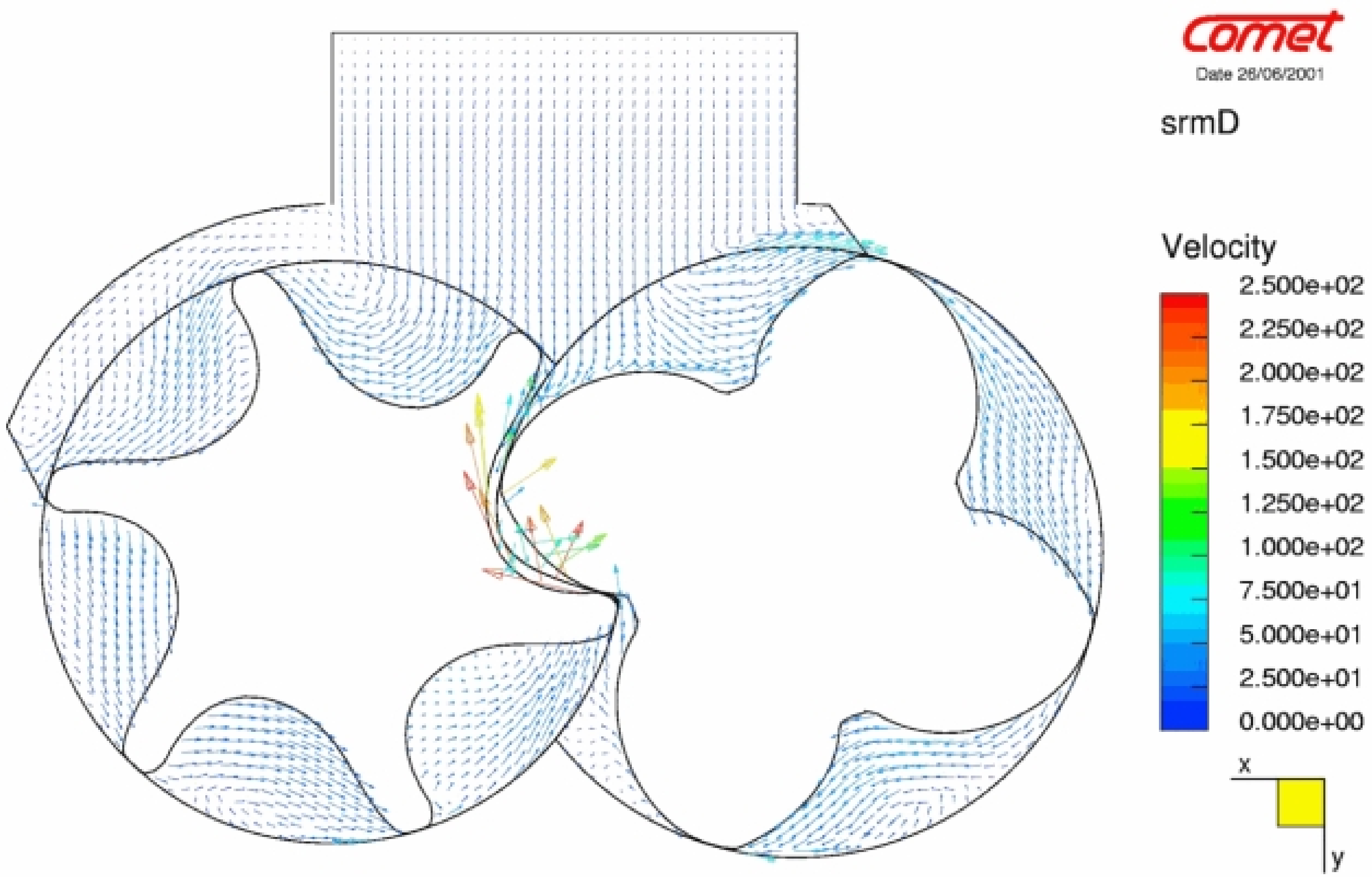

Dry compressor – velocities in X plane

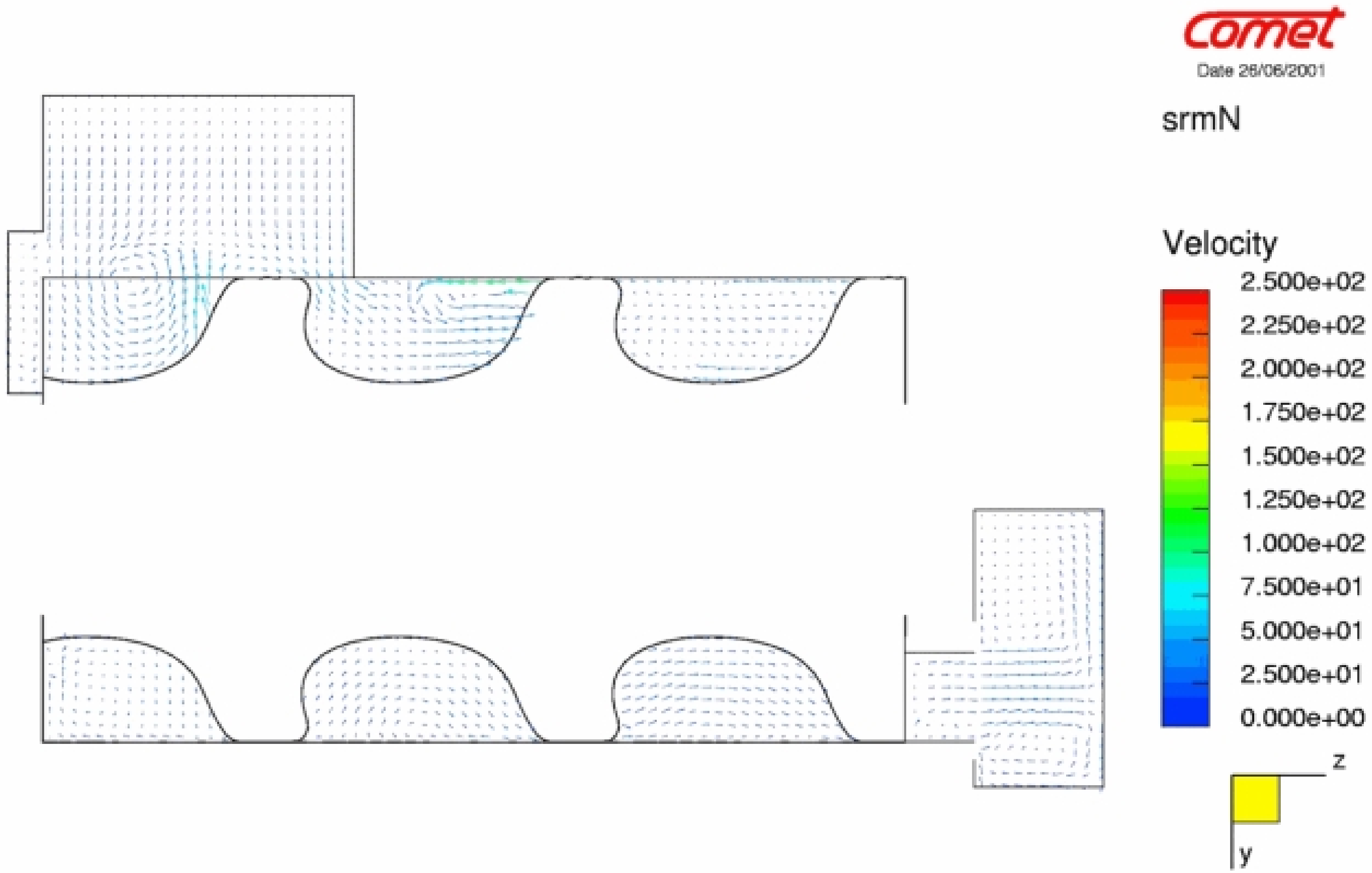

Dry compressor – pressure

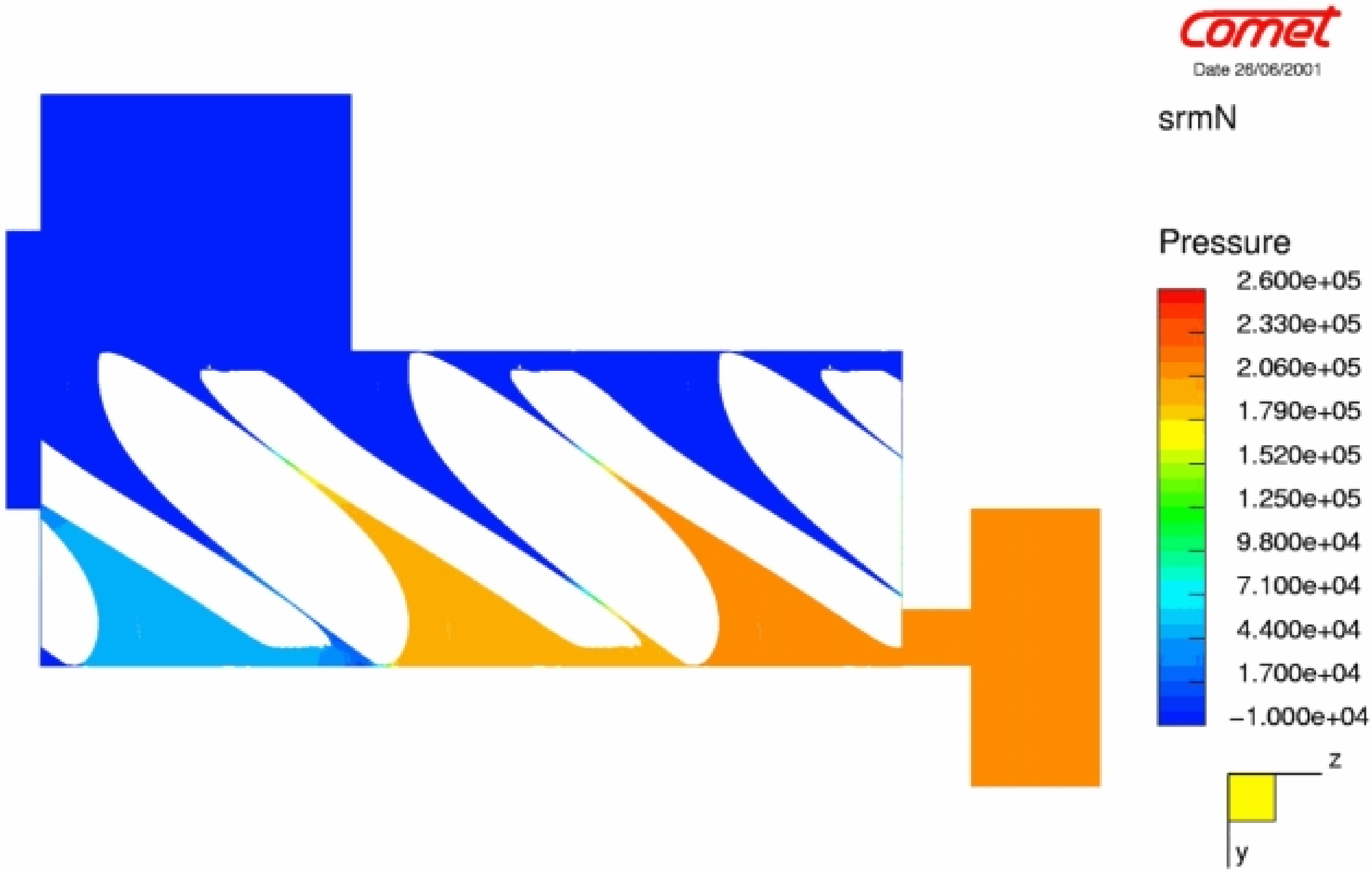

Dry compressor – temperature

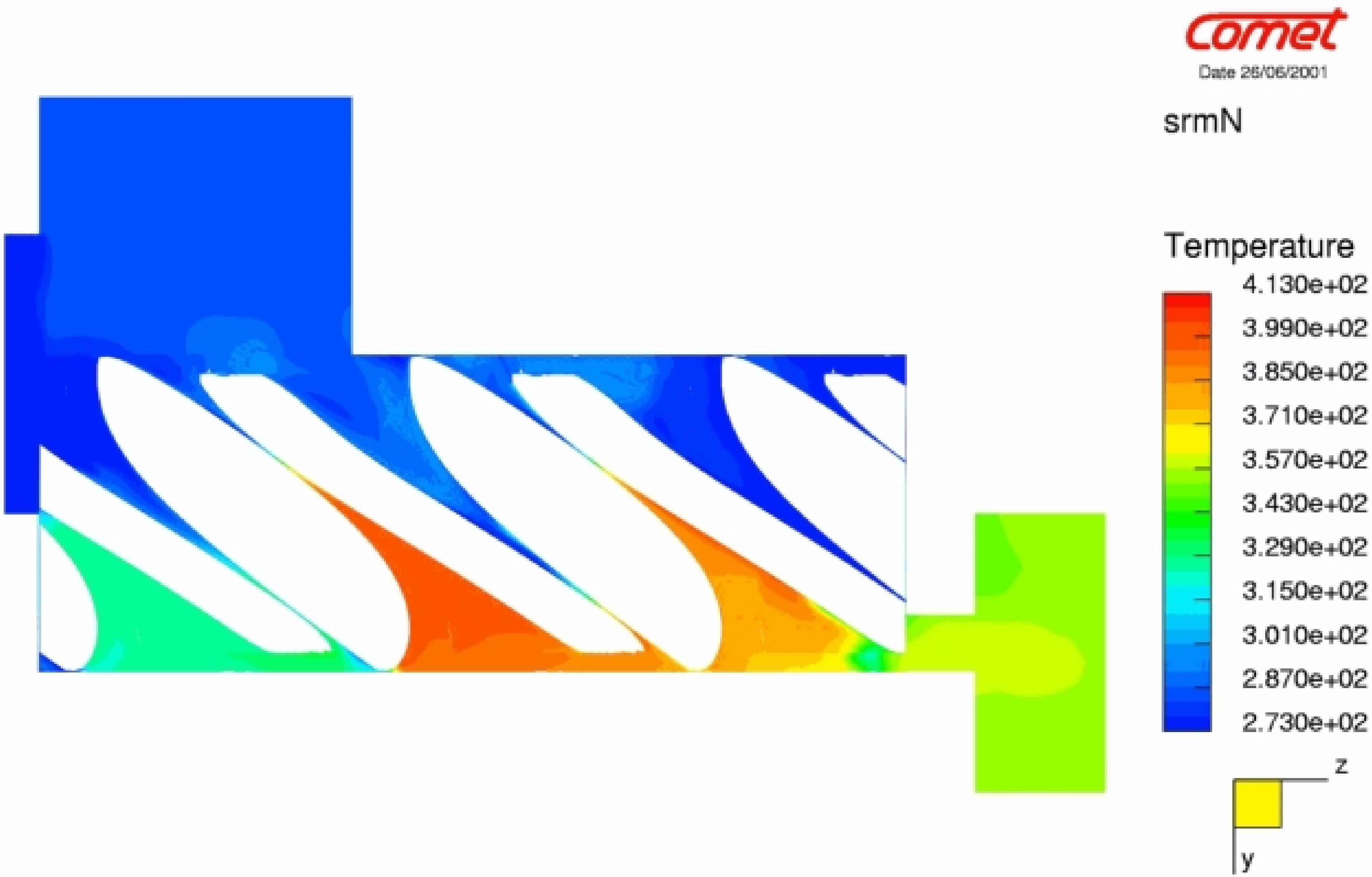

Dry compressor - comparison

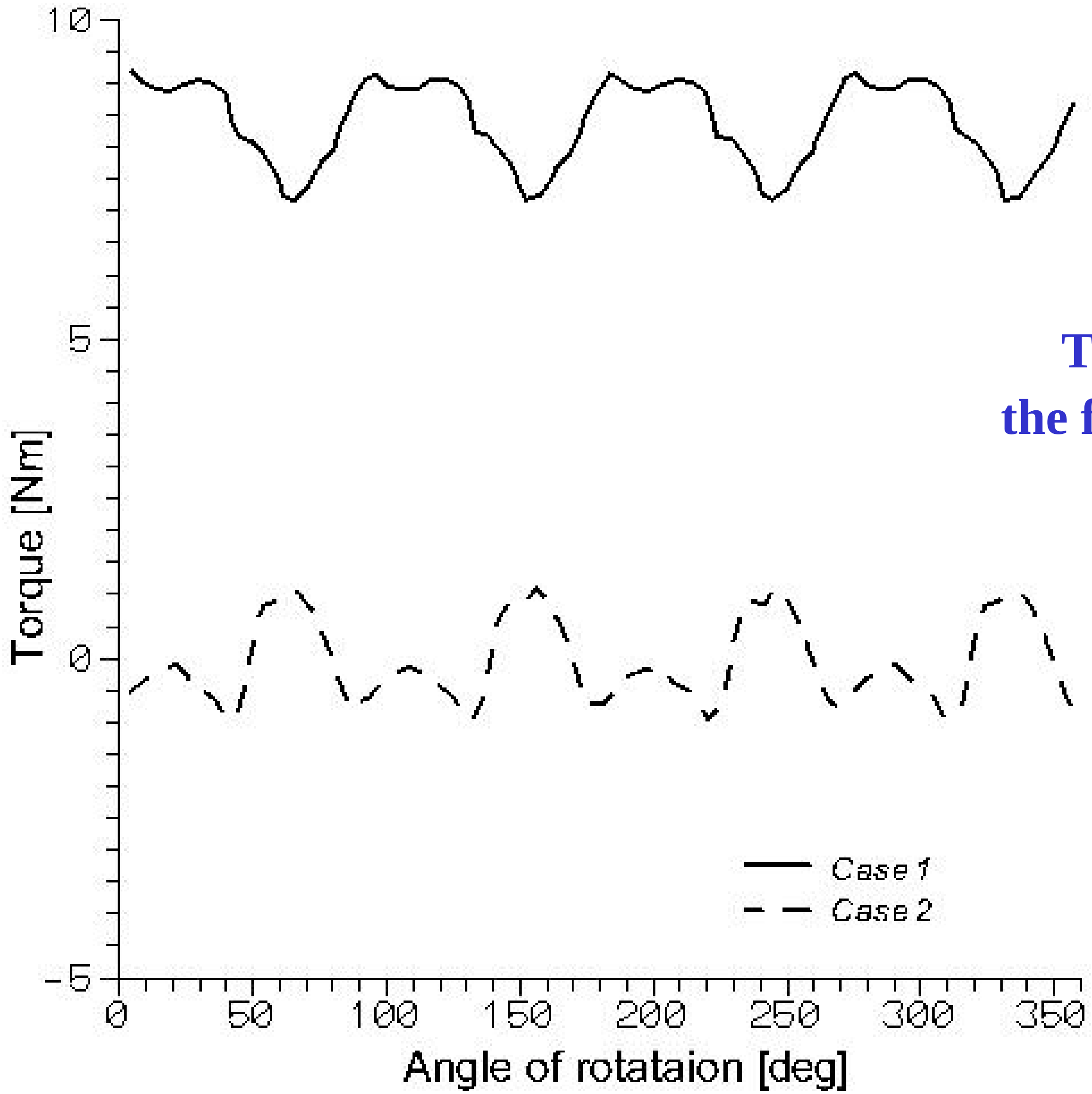

Torque on the female rotor

Oil injected air screw compressor

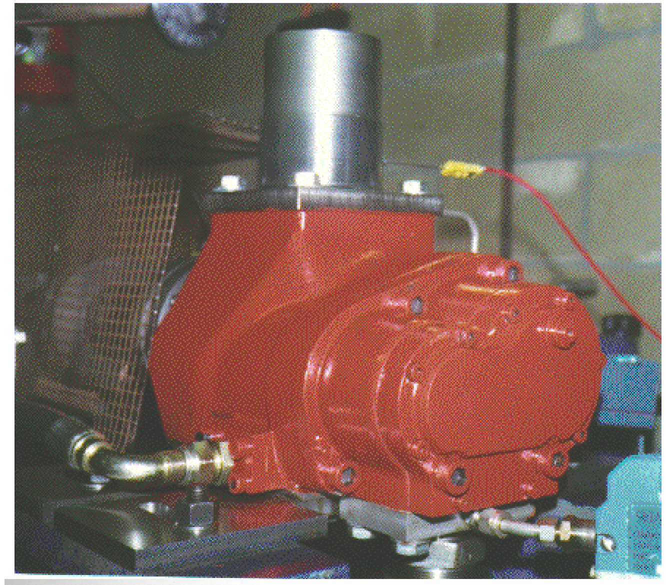

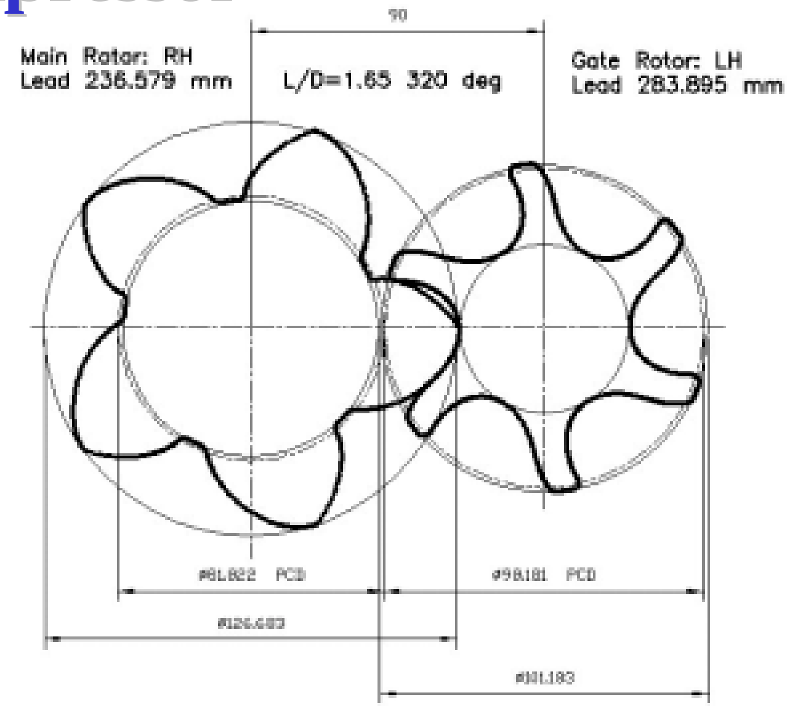

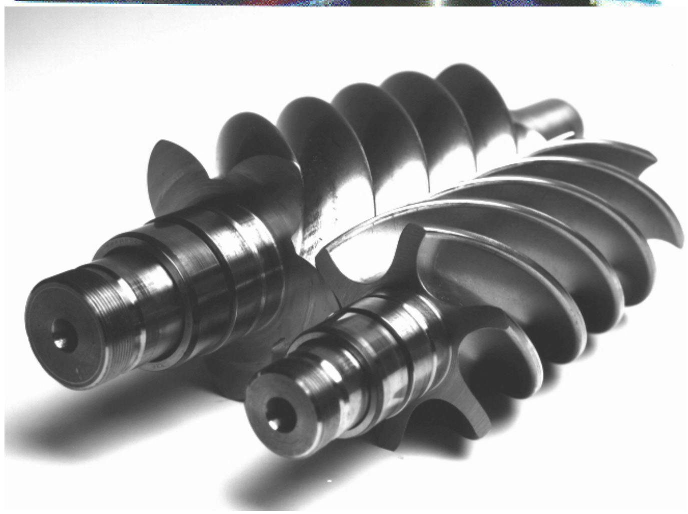

Configuration 5/6

d_1= 126.683 mm, d_2= 101.383 mm, a= 90 mm

l=212 mm, l/d=1.66, wrap=320 deg

Clearances **50** μm

Speed 5000 rpm, P_{inl}= 1 bar, P_{out} = 6, 7, 8, 9 bar

442 130 cells, 25 time steps/cycle

Oil injected - Pressure in axial section

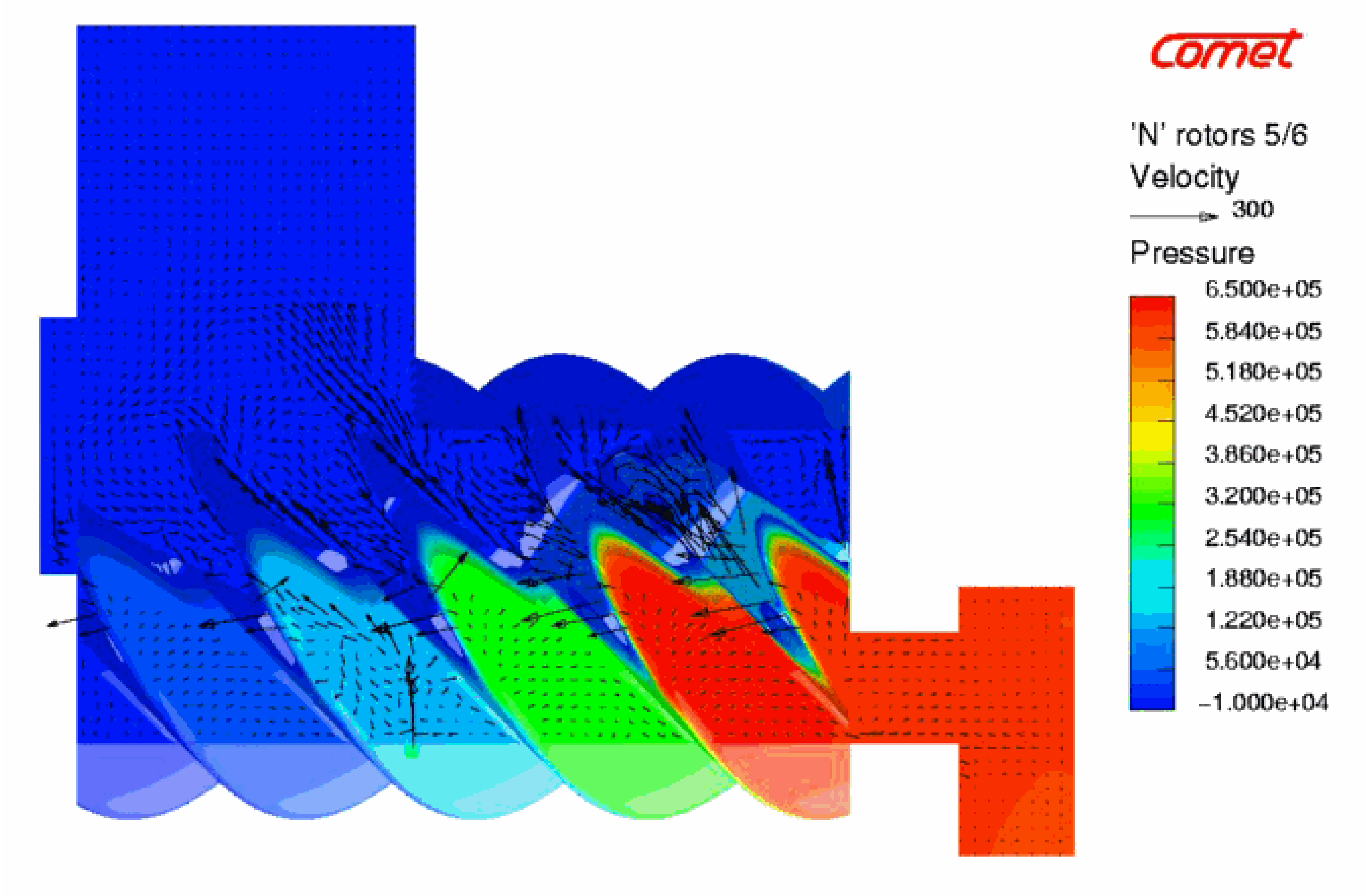

Oil injected - Pressure and velocity

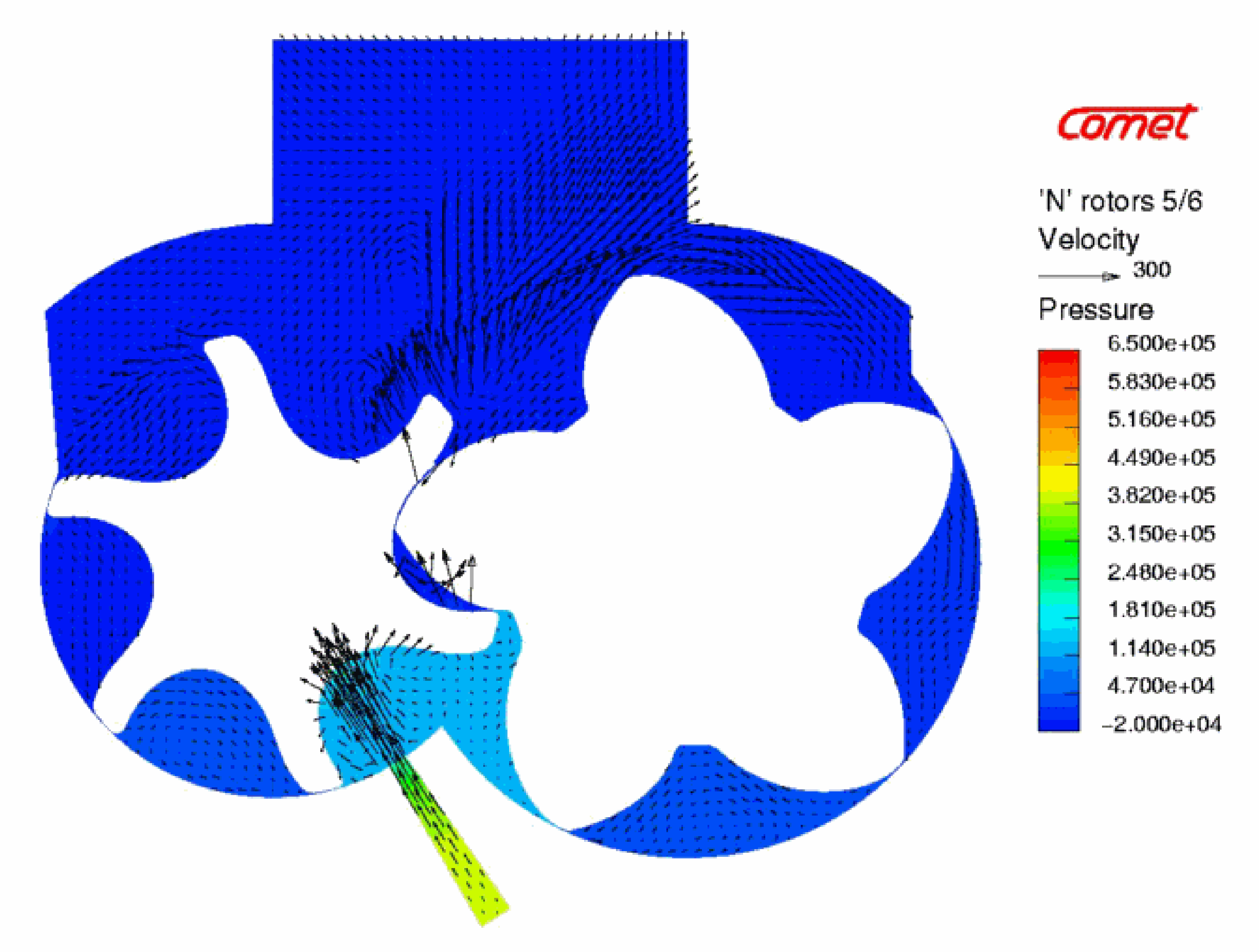

Oil injected - Pressure 3D view

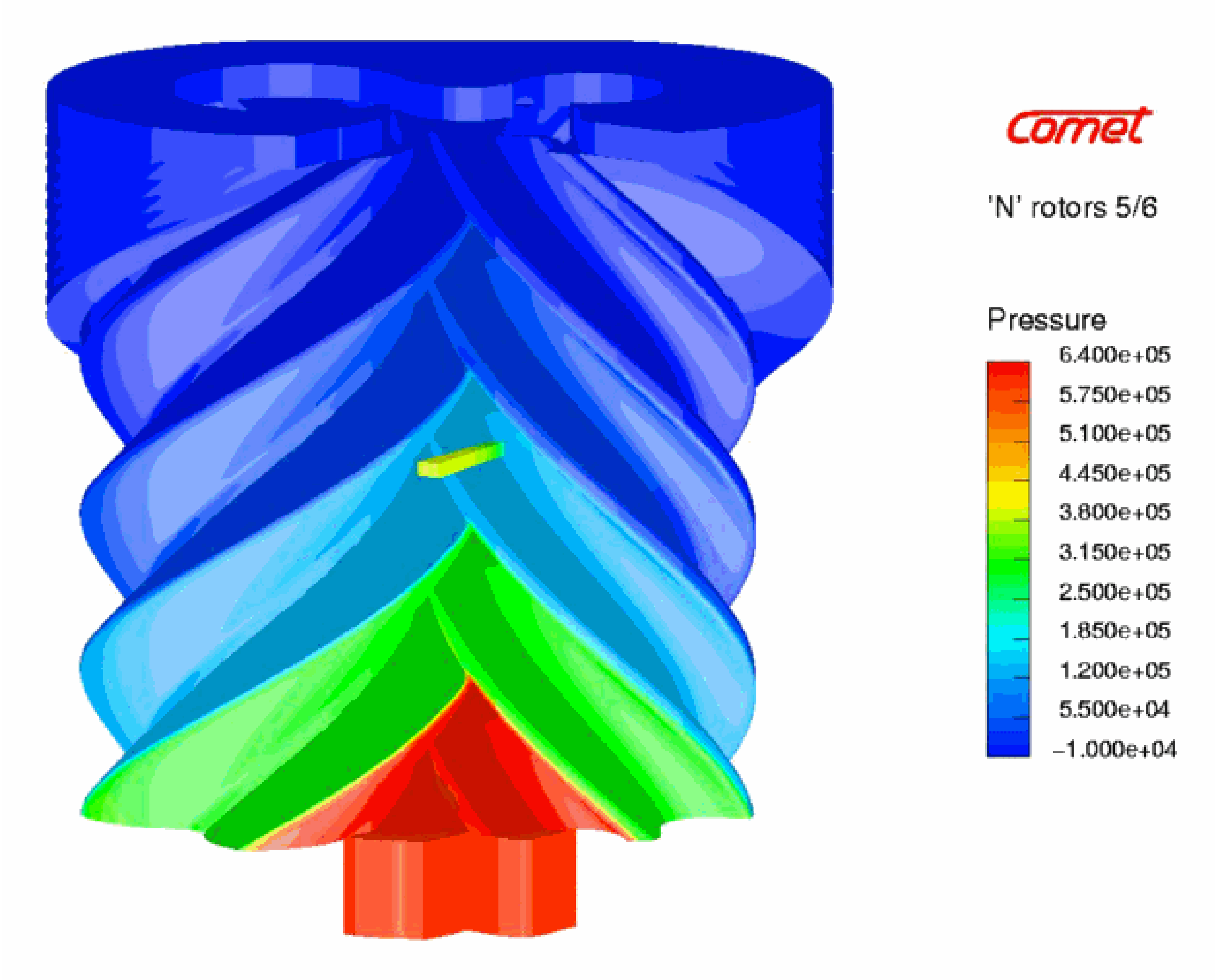

Oil iniected - Oil concentration in cross section

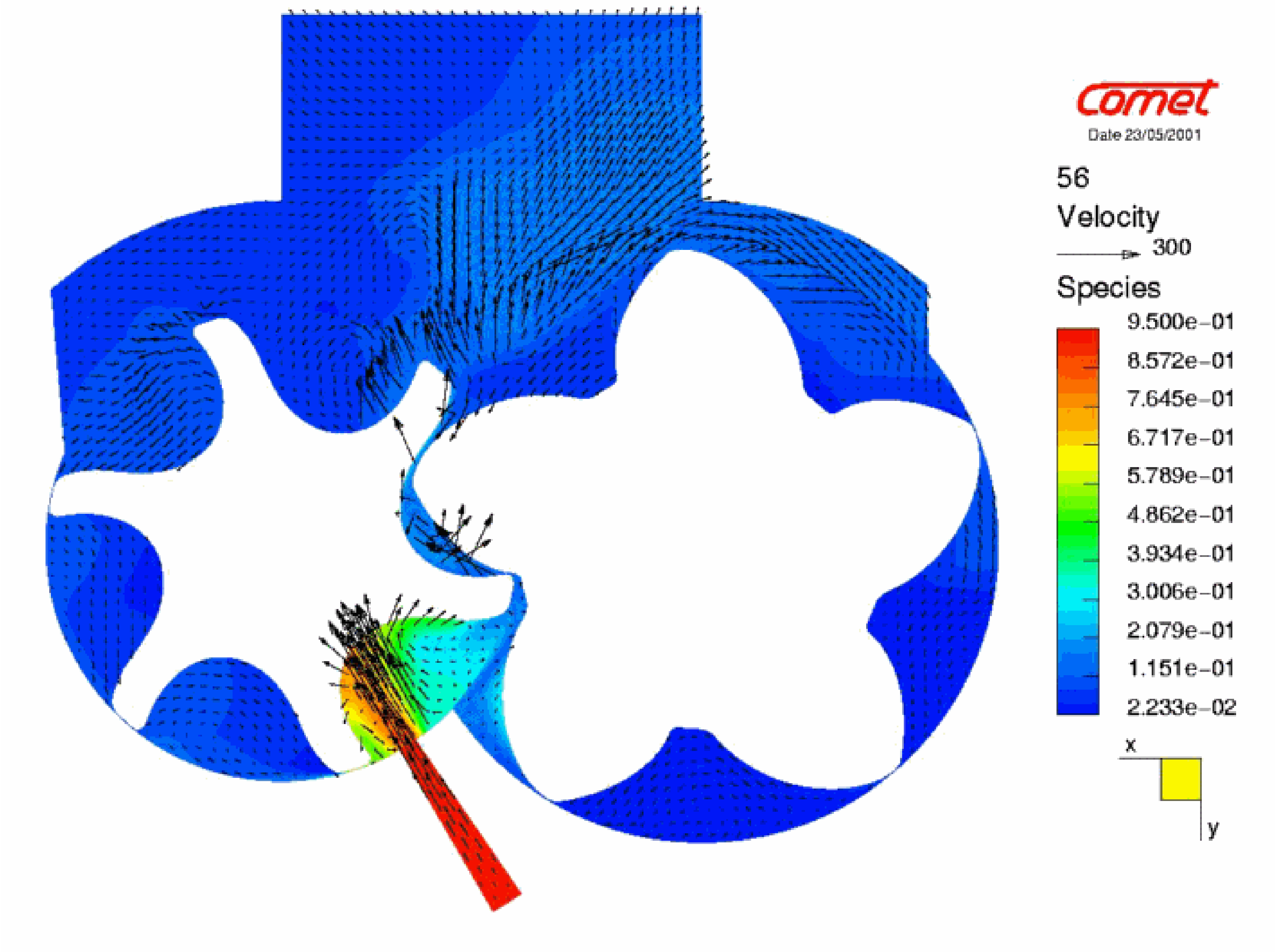

Oil injected - Oil distribution 3D view

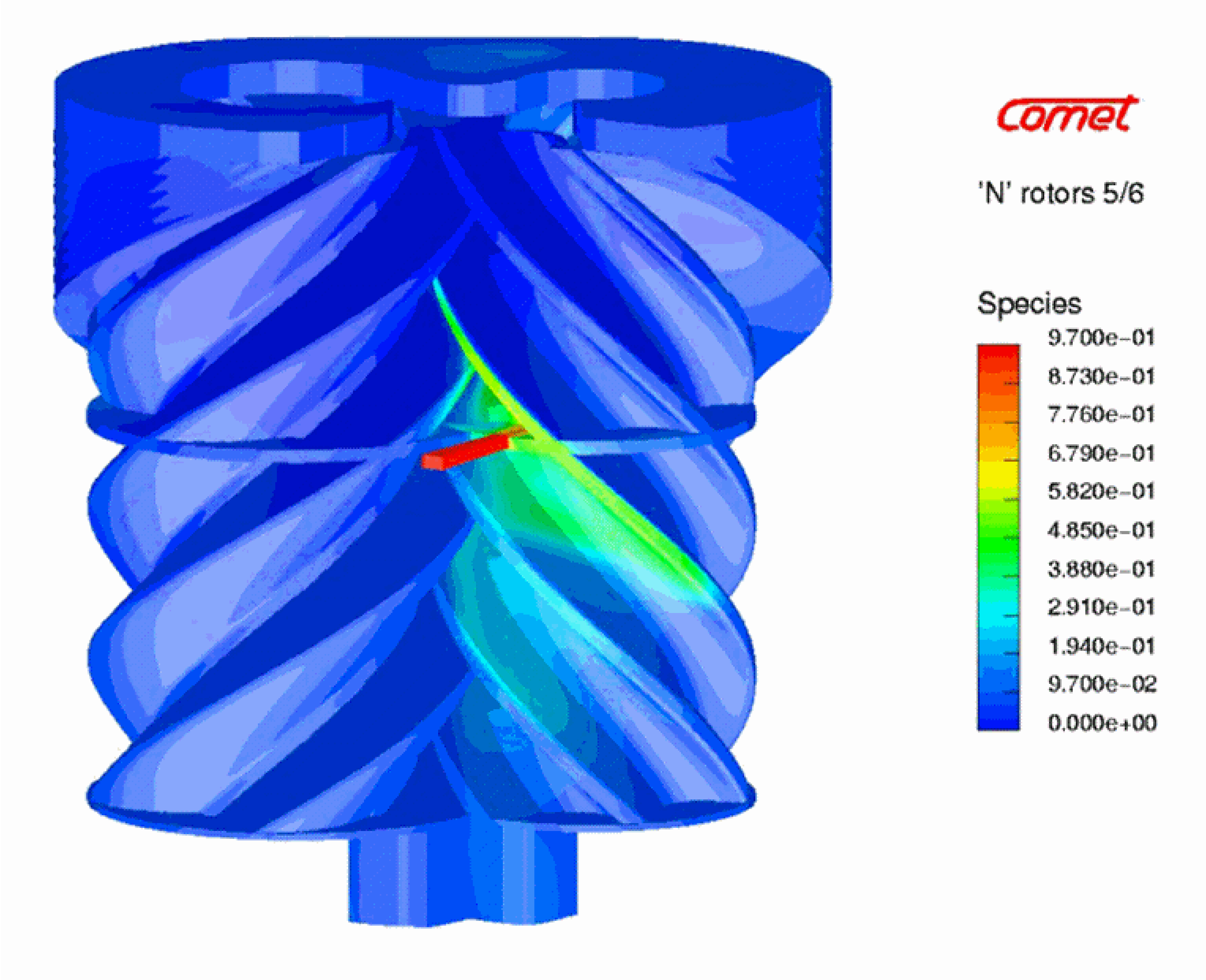

City University London

Experimental verification

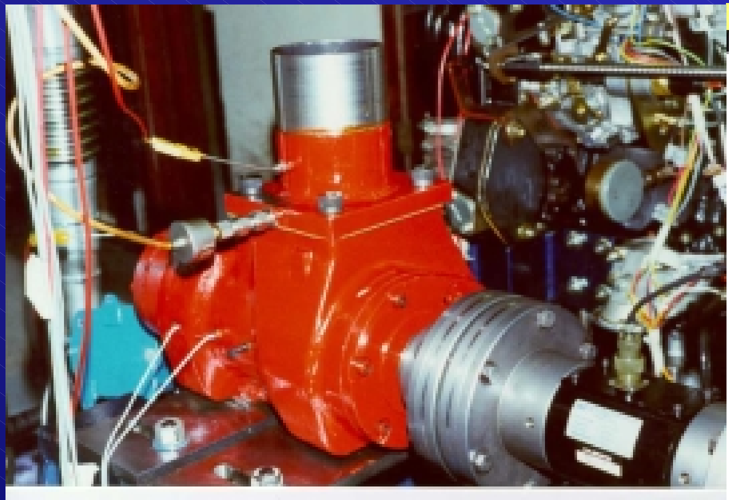

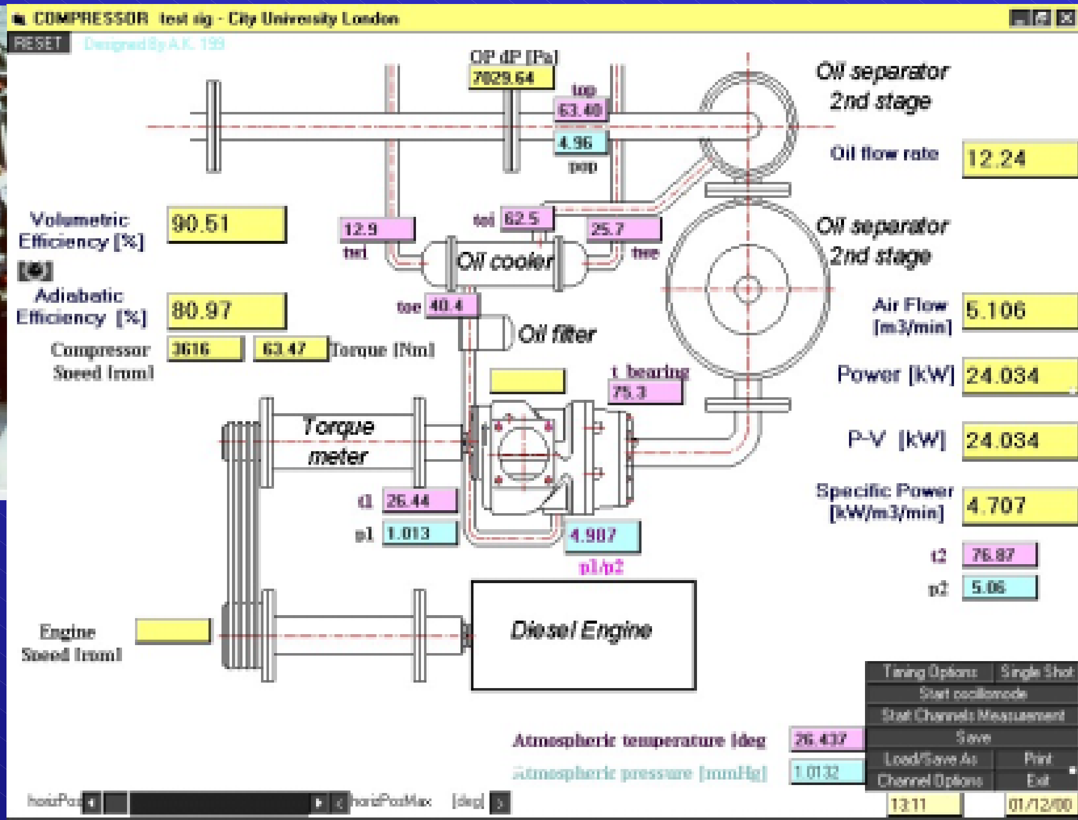

-Test rig enables oil flooded and dry air compressors to be measured. Limits:
- Power <= 100 kW
- Delivery <= 16 m^3/min

- High accuracy test equipment
- p-α diagram – piezoelectric transducers
- Computerized data logger
- Real time calculation and presentation

- Meets Pneurop/Cagi standards
- Compressor tested to ISO 1706
- Flow measurements BS 5600
- Certified by Lloyd's of London

Experimental verification – P-α diagram

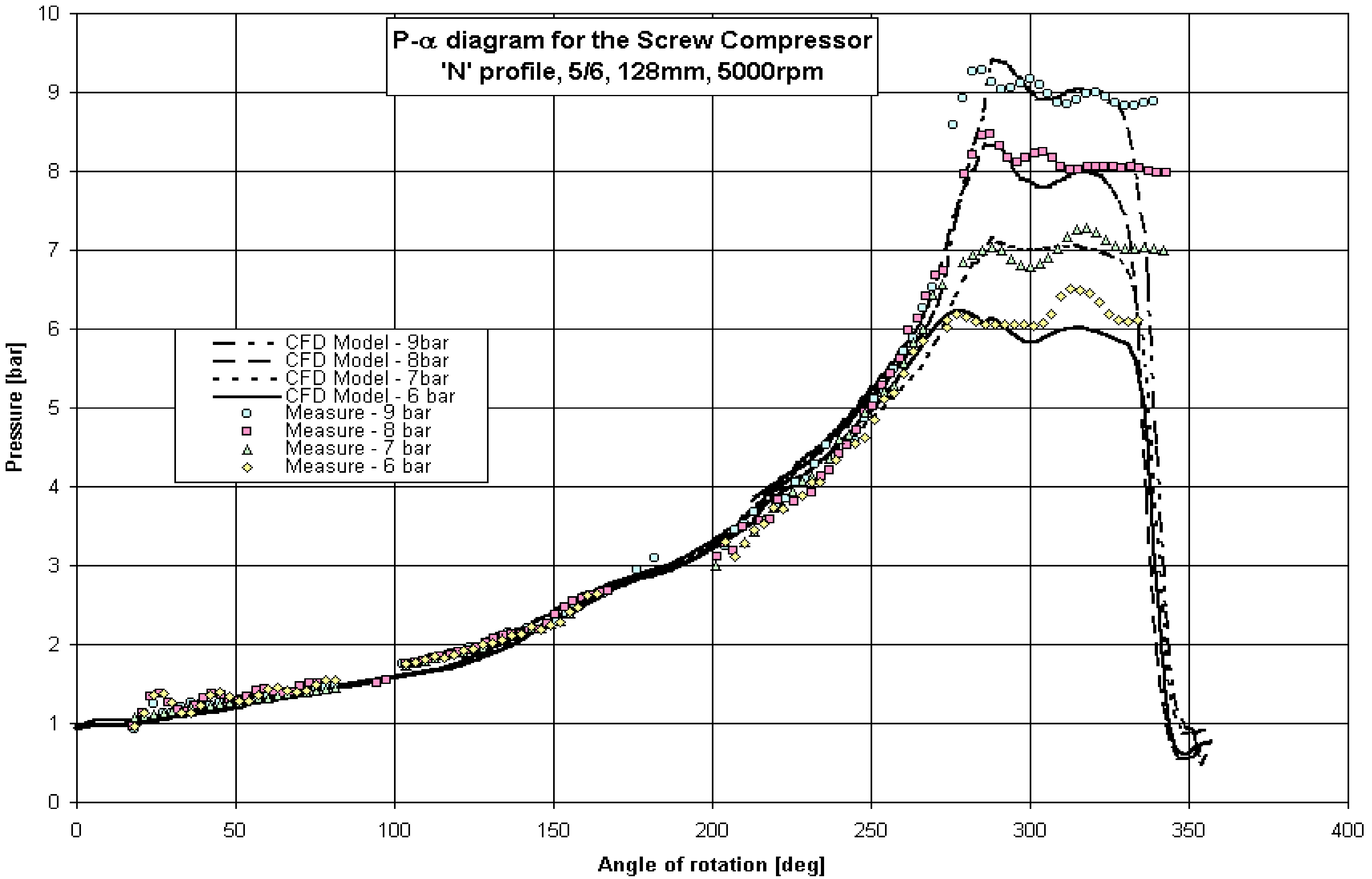

Integral parameters – Torque

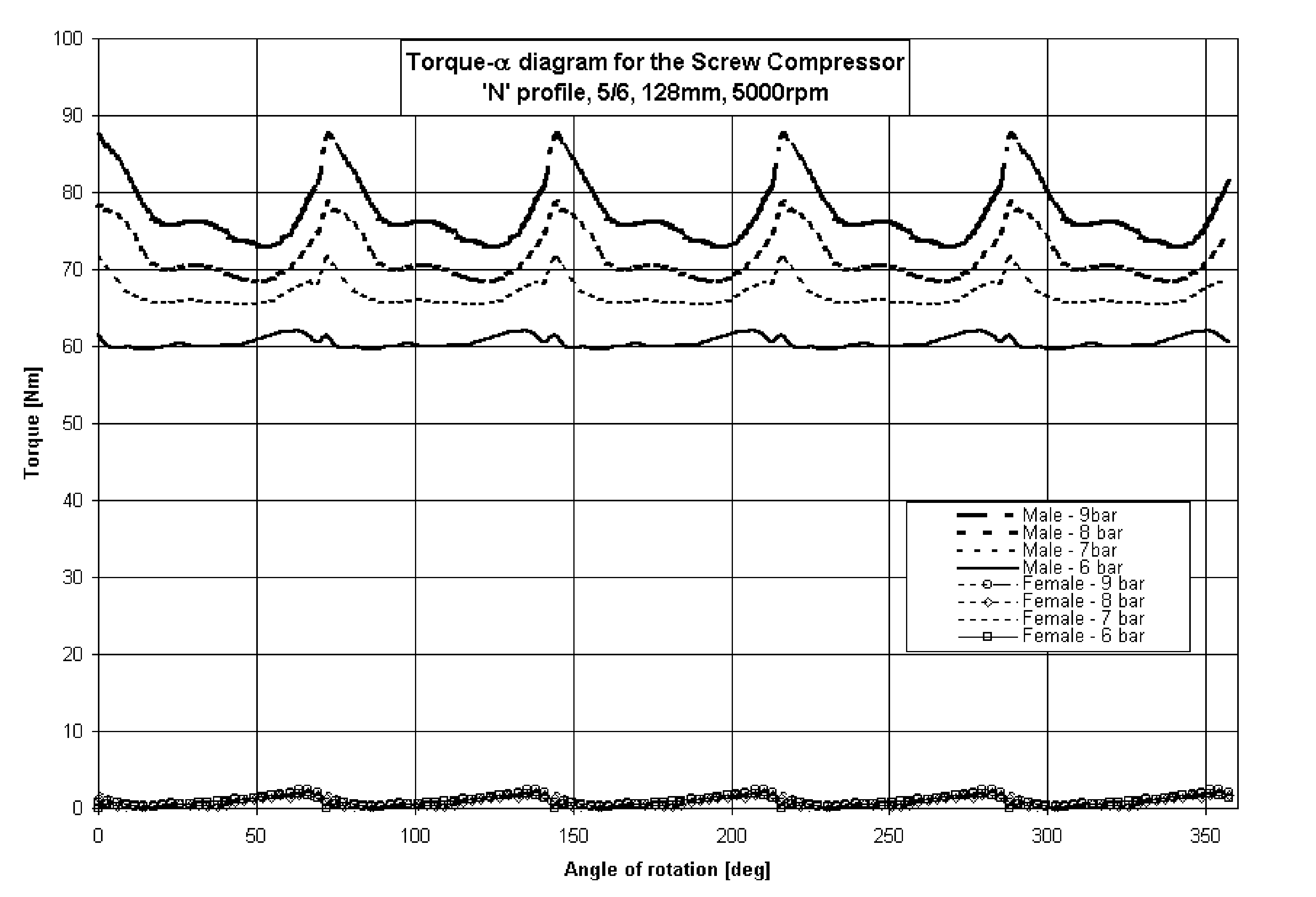

Integral parameters – Power, Delivery

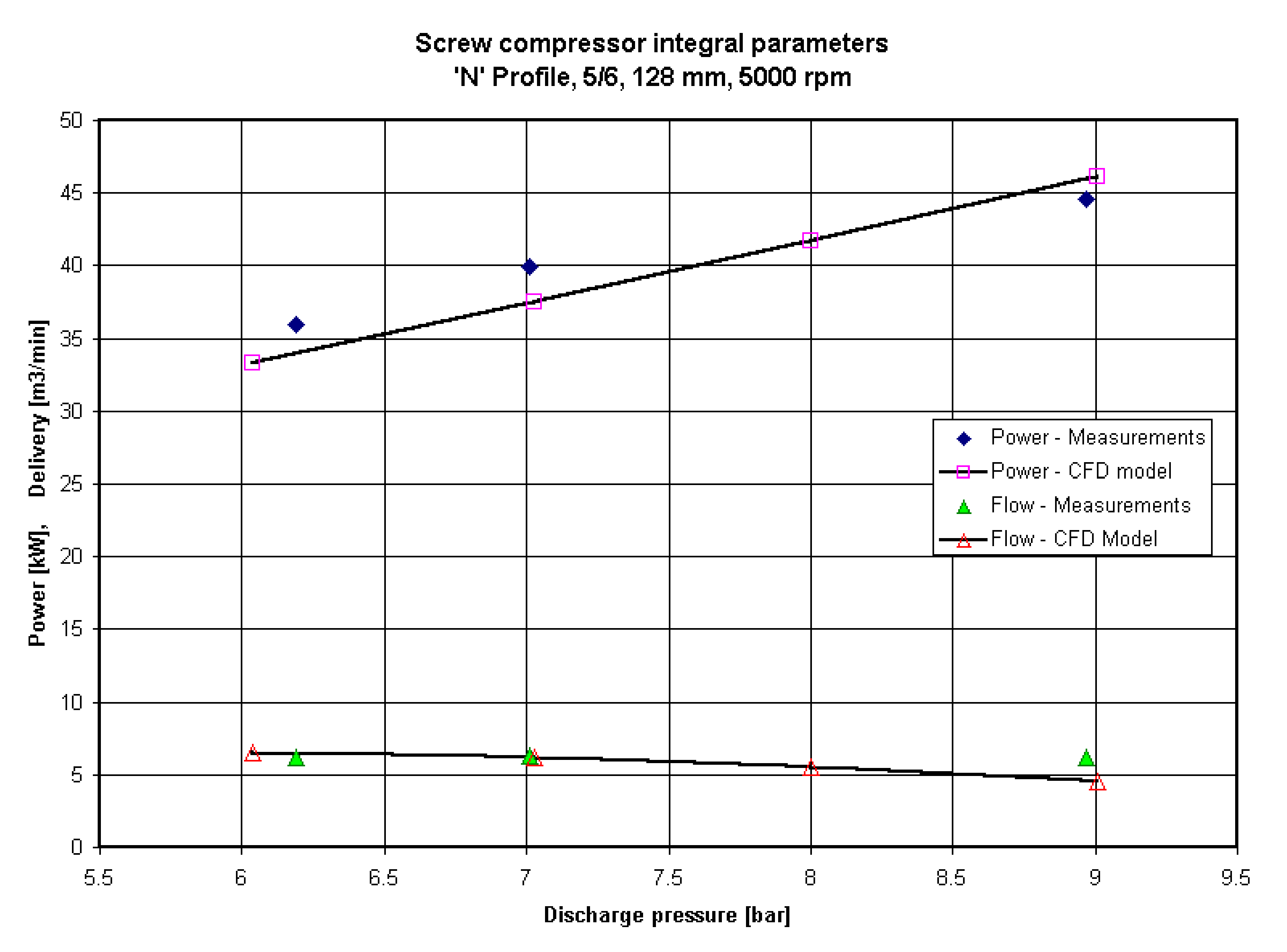

Oil injected compressor real fluid - Ammonia

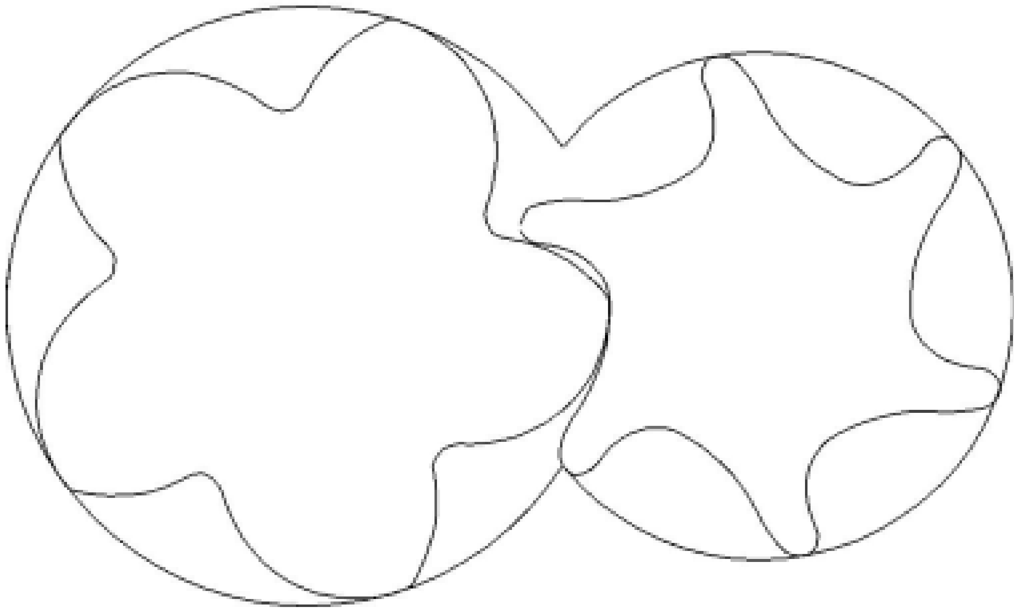

Configuration 5/6

d_1= 144.43 mm, d_2= 121.92 mm, a= 108.306 mm

l=200 mm, l/d=1.384, wrap=216 deg

Clearances 100 µm

Speed 5000 rpm, P_{inl}= 1 bar, P_{out} = 7, 9 bar

256 690 cells, 20 time steps/cycle

Real fluid - Ammonia - pressure

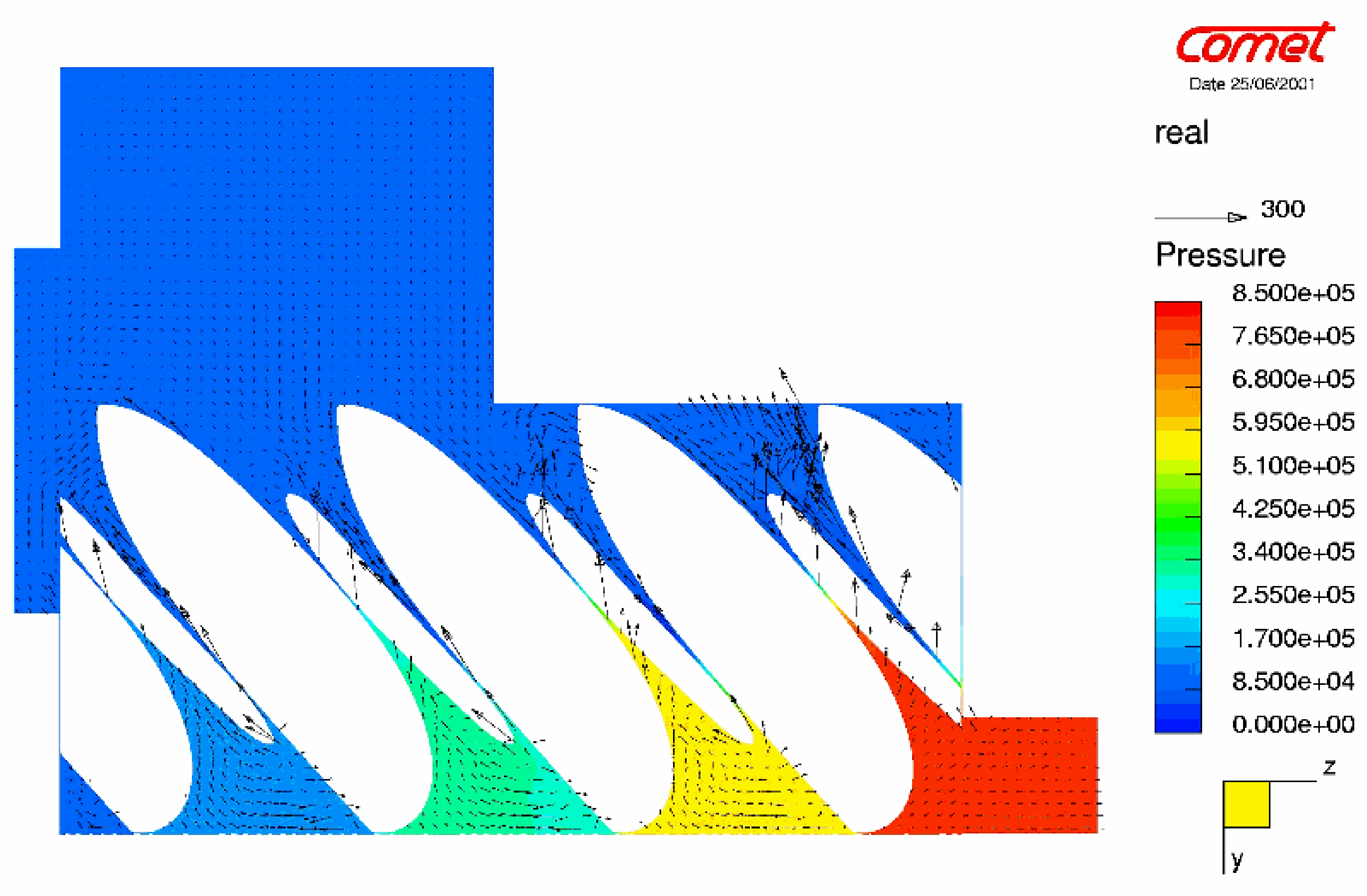

Real fluid - Ammonia – pressure

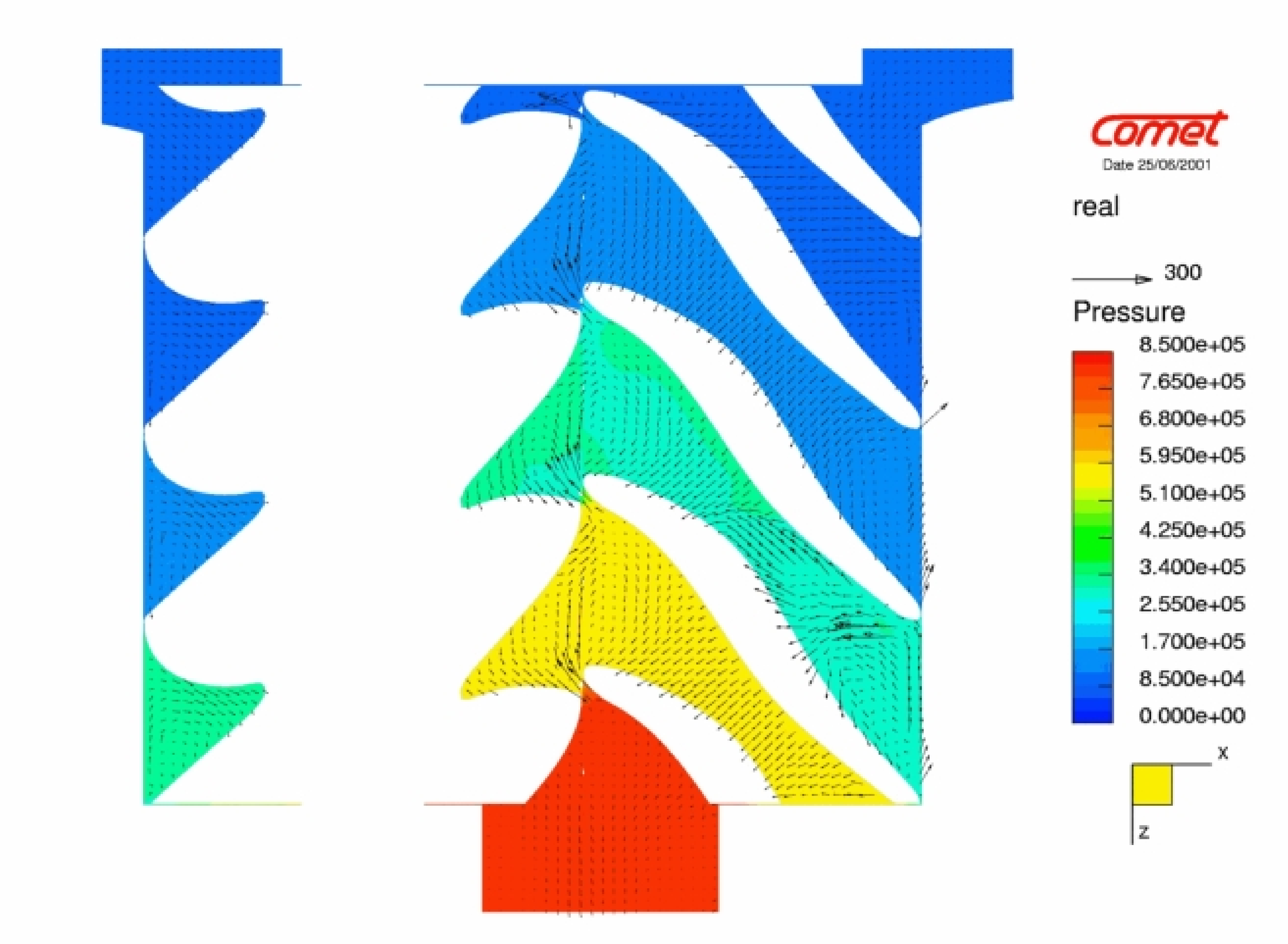

Real fluid - Ammonia - pressure

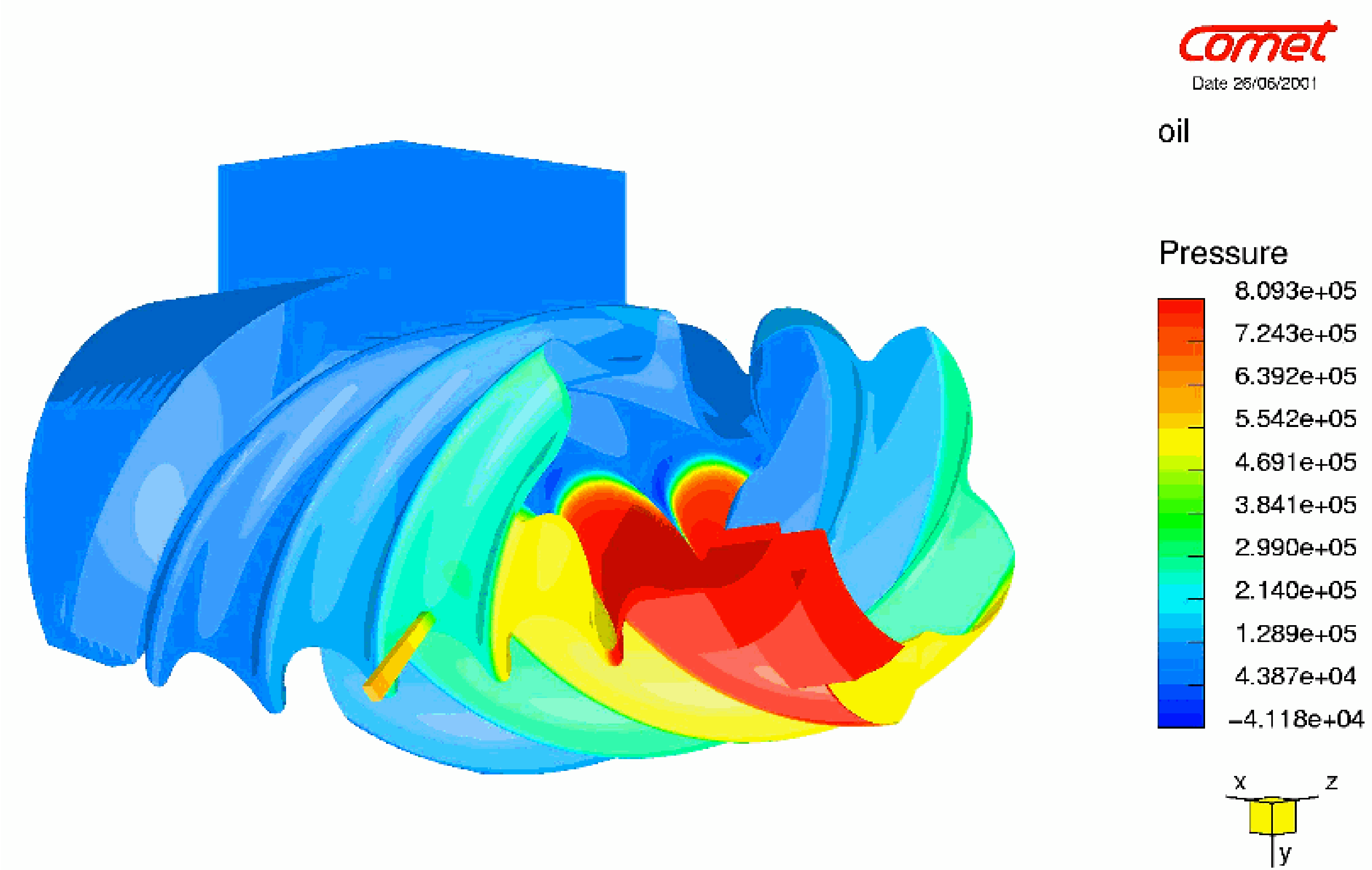

Real fluid - Ammonia - oil in the cross section

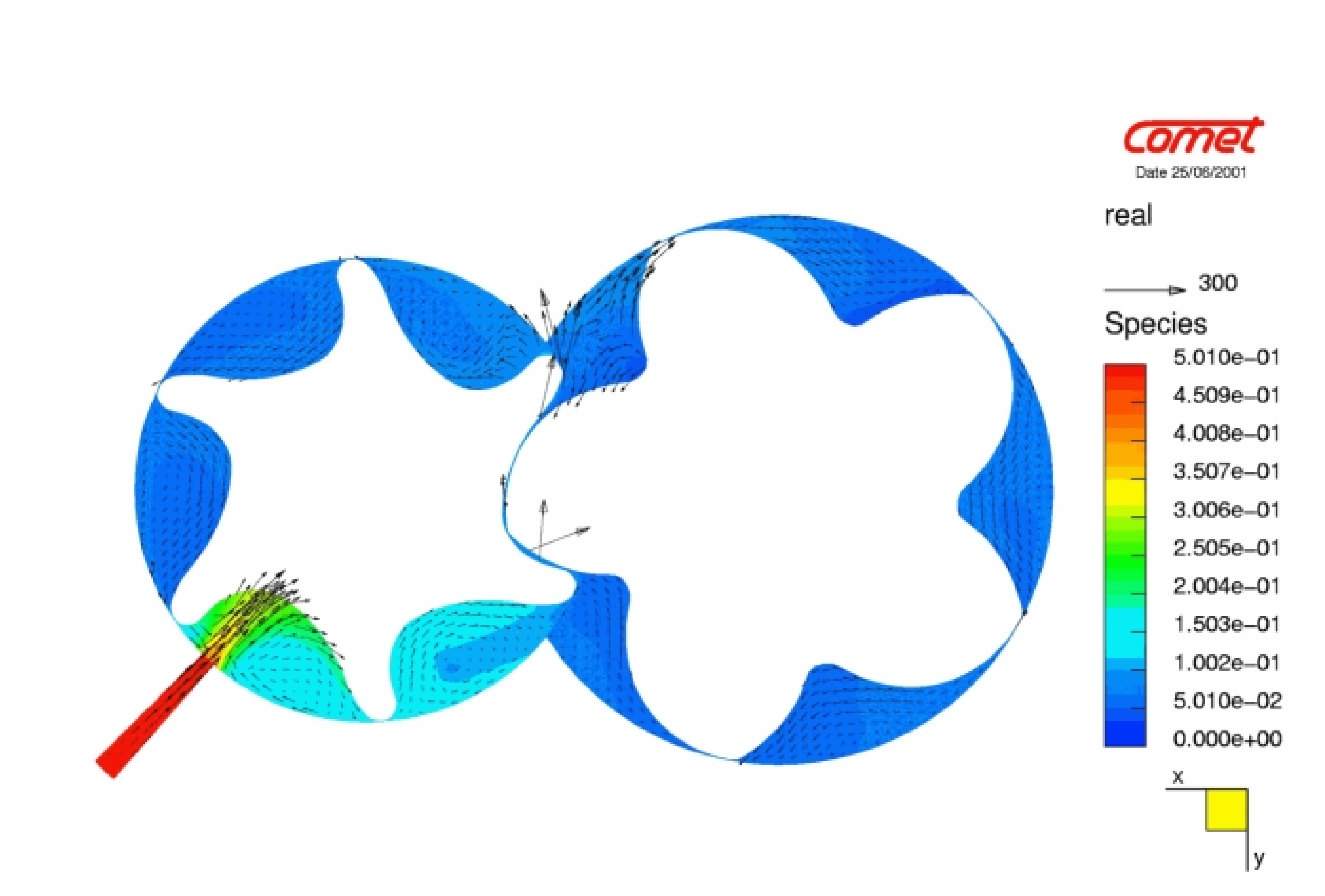

Real fluid - Ammonia - oil distribution

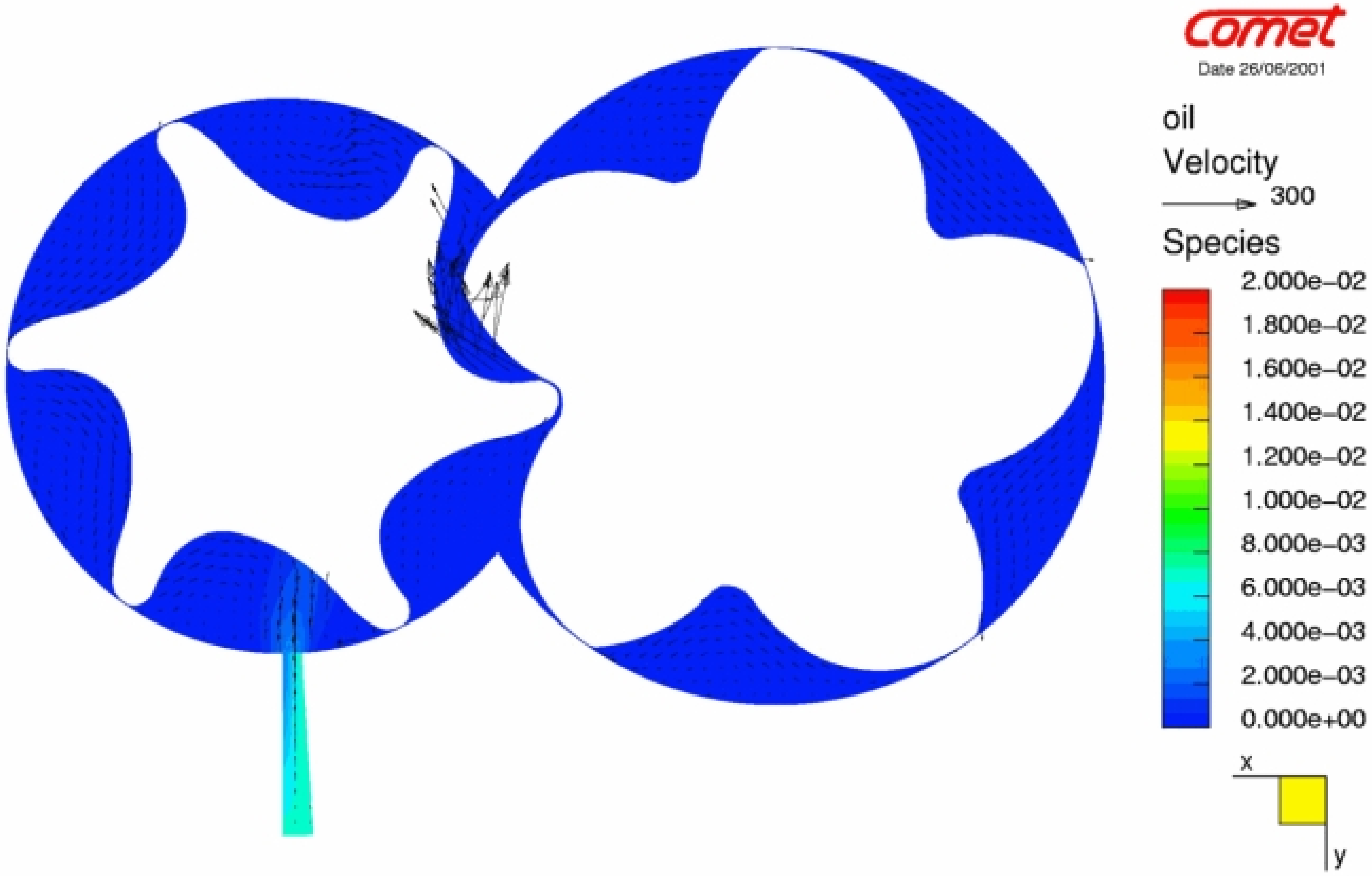

Real fluid - Ammonia - oil distribution

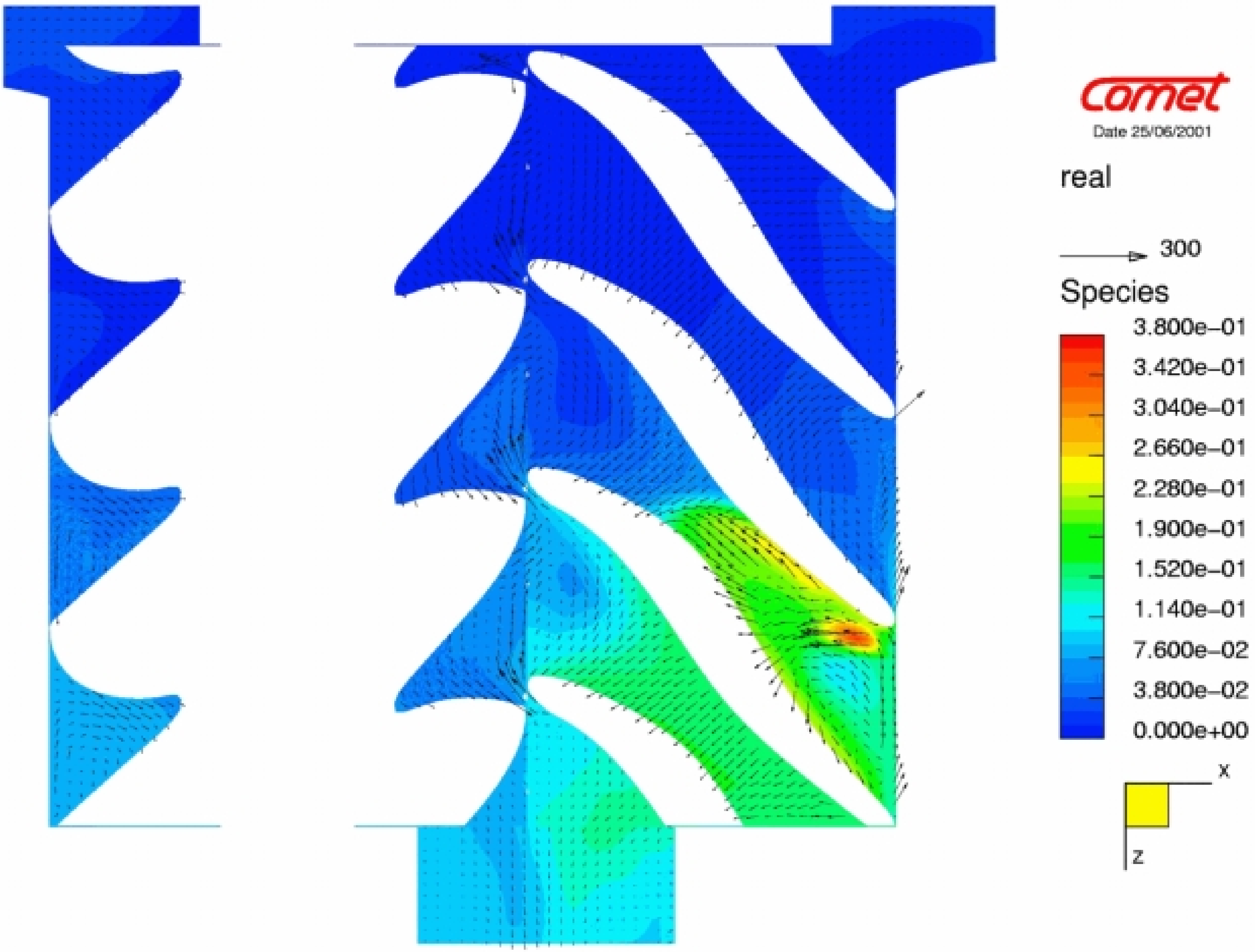

City University London

Real fluid - Ammonia - oil distribution

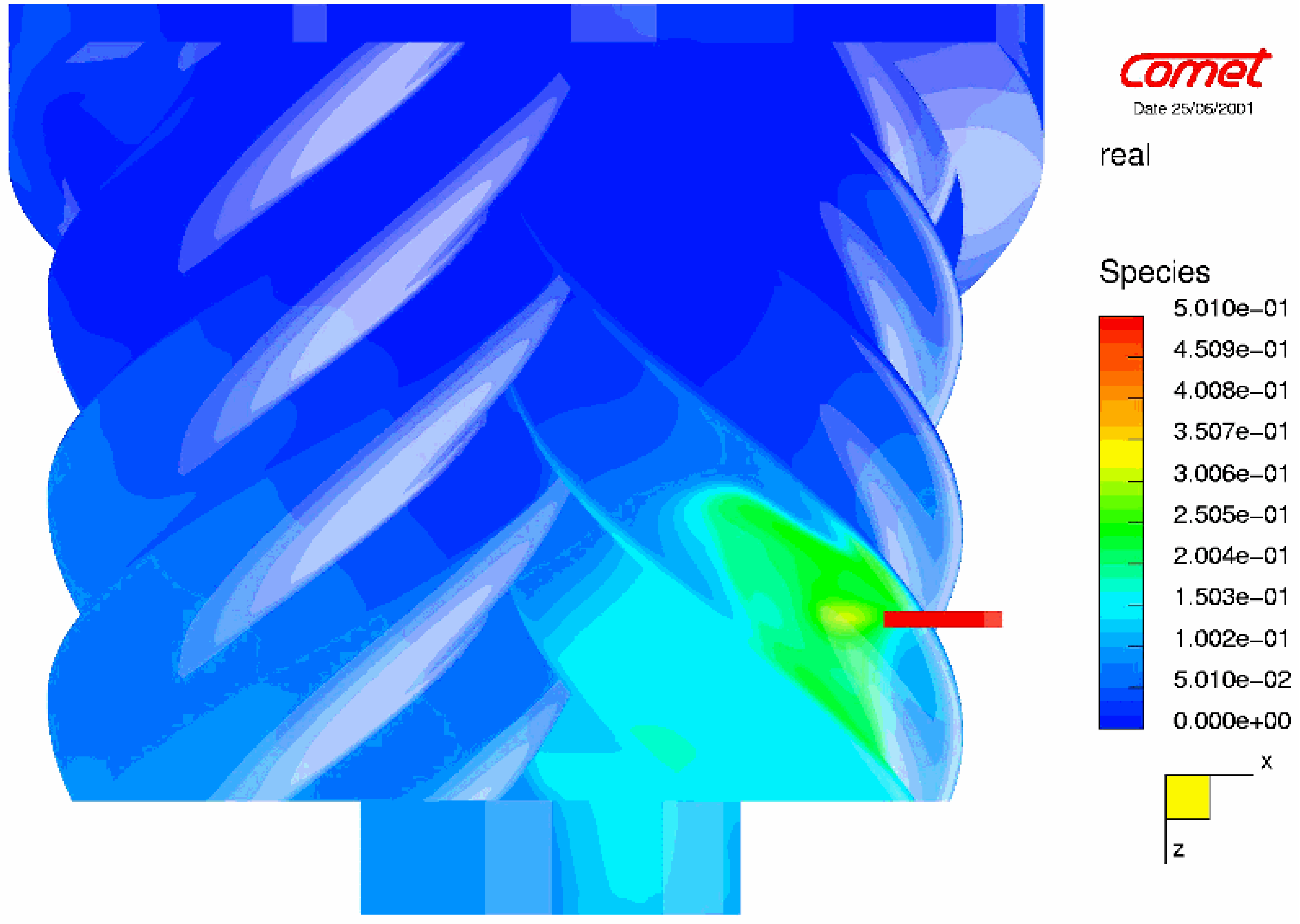

Real fluid - P-alpha diagram

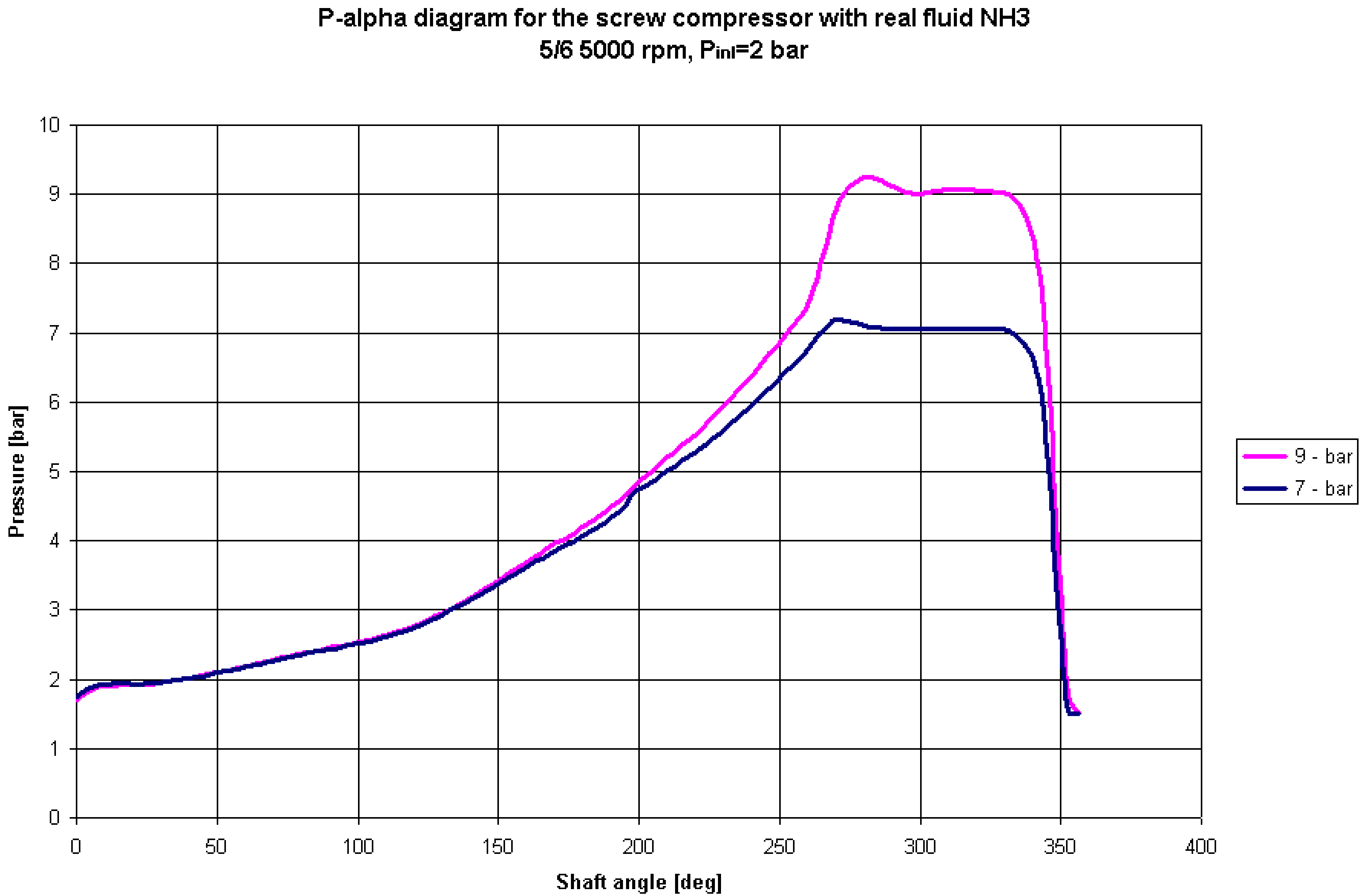

City University London

Real fluid – Torque and delivery

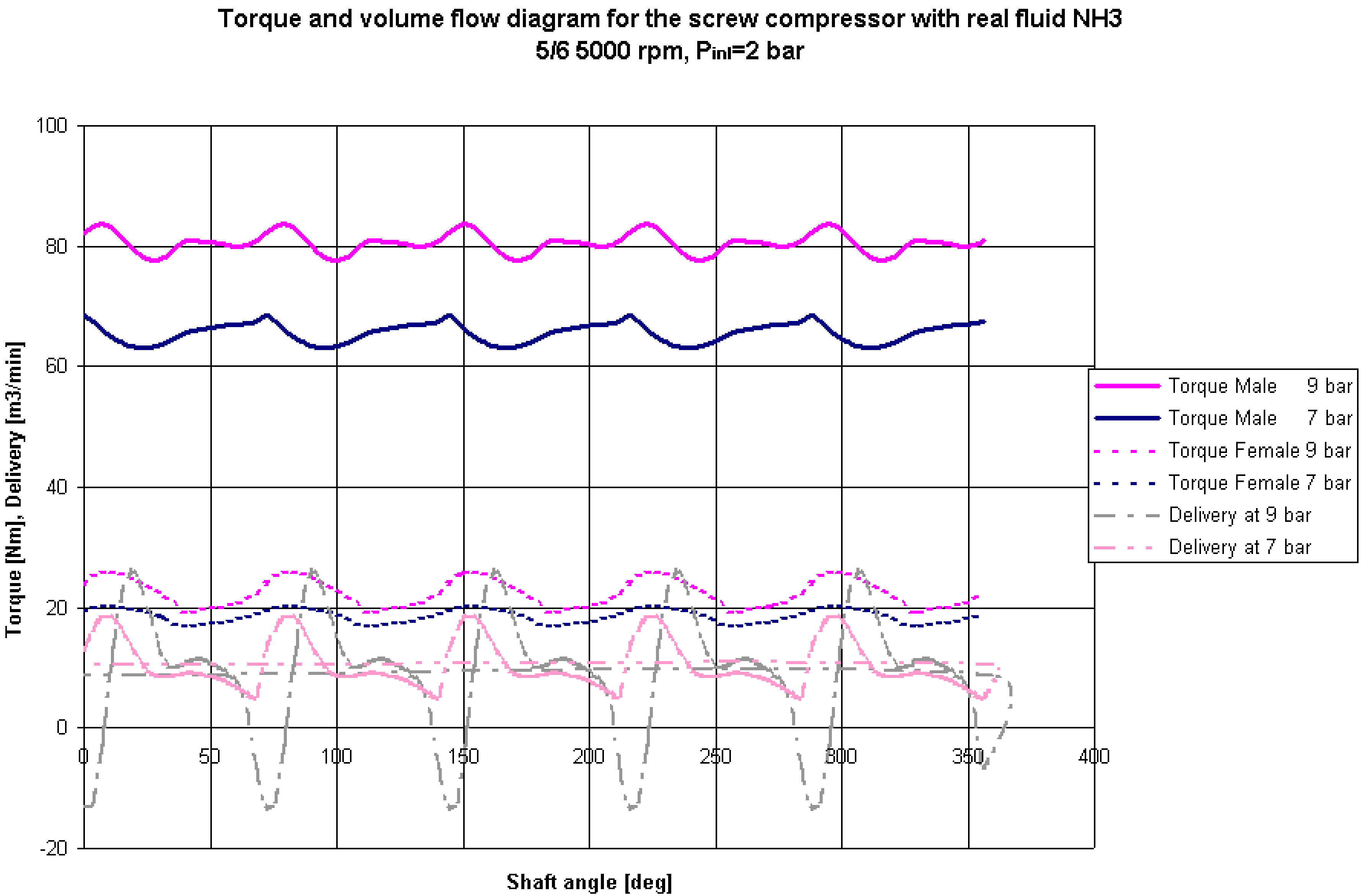

Two phase screw expander

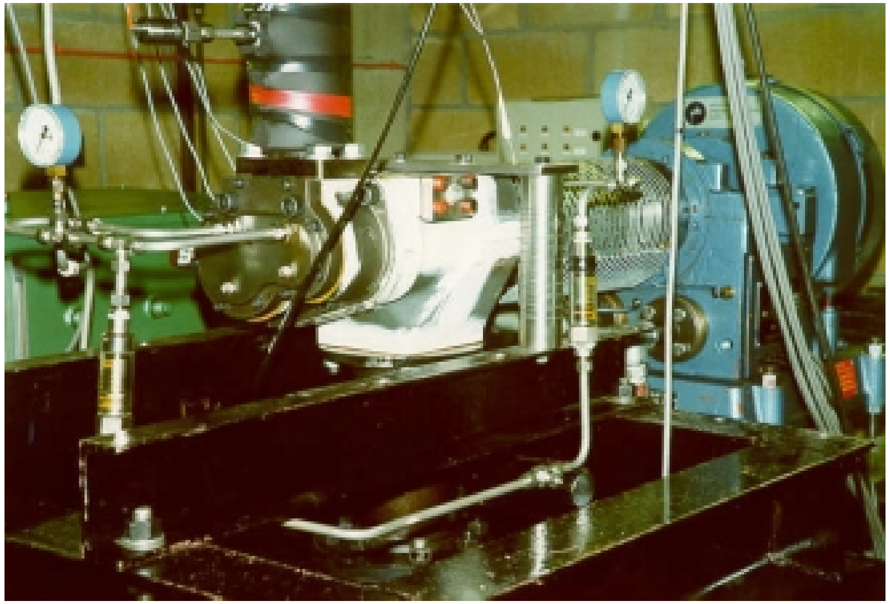

Working fluid R-113

Configuration 5/6, d_1= 126.683 mm, d_2= 101.383 mm, a= 90 mm
l=212 mm, l/d=1.66, wrap=320 deg
Clearances **100** µm
Speed 2000 rpm, P_{inl}= 8 bar, T_{inl}=126 degC, x_1=1
P_{out} = 4 bar, T_{out}=87 degC, x_2=0.2

266 650, 20 time steps/cycle

Expander – liquid concentration

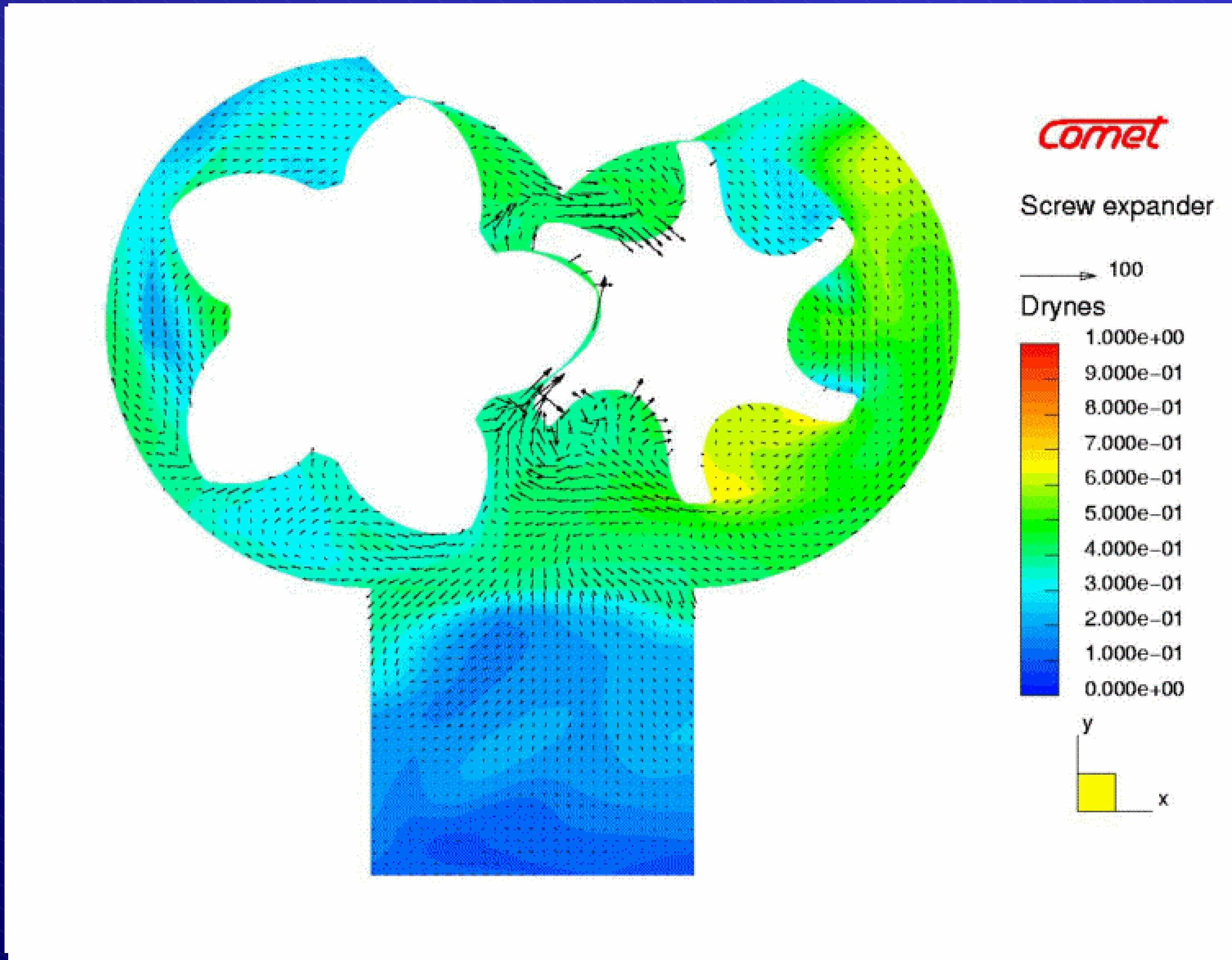

Expander – p-alpha diagram

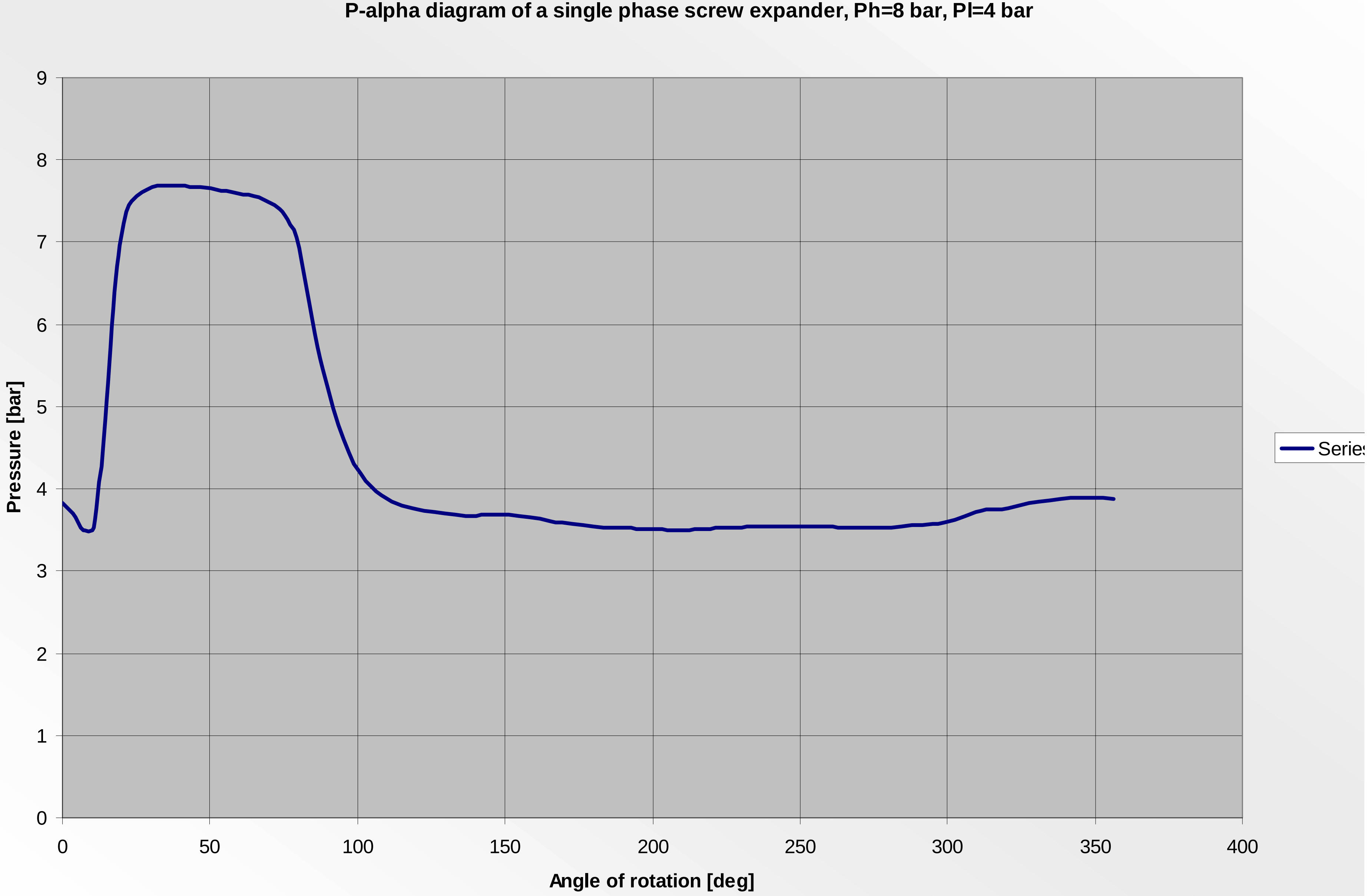

CONCLUSIONS

- A method for 3-D calculation of twin screw machines has been developed which is valid for any CFD solver that meets specified requirements.
  - Adaptive analytical transfinite interpolation with orthogonalization, smoothing and regularity check has been used to generate a 3-D structured numerical grid;
  - Multi-phase flow simulation and novel approach to boundaries can be incorporated in any CFD solver through user functions;
- *SCORG* - A stand alone CAD-CFD program developed to transfer screw compressor geometry and parameters to CFD solver automatically;
- *COMET* **GMBH** ICCM was used for calculation and post-processing;
- Integral parameters calculated on the basis of CFD results;
- Results are compared with measurements obtained on certified air compressor test rig;
- Good agreement achieved, method is verified.

EPILOGUE

- City University, London is the world leader in the application of Computational Fluid Dynamics to screw compressor design.
- Adaptive meshing and transfinite interpolation with orthogonalization and smoothing are employed to generate a grid which takes advantage of the innovative techniques in contemporary finite volume numerical solvers.
- Flow situations, which involve stretching and sliding rotor domains and geometry with large variations in scale and moving grids are solved efficiently.
- New procedures have been implemented in the CFD solver program through user functions to greatly increase the speed of calculation.
- Results of such calculations compared with experimental test data show good agreement with the measured values.